

ARTEMIS

Validation Manual

Version v8p5
December 1, 2023



Contents

1	Energy loss due to wave breaking: BJ78	6
1.1	Purpose	6
1.2	Description of the test case	6
1.2.1	Geometry	6
1.2.2	Mesh	6
1.2.3	Boundary conditions	6
1.3	Reference solution	7
1.4	Results	8
2	Transformation of a wave on a circular bump: bosse	10
2.1	Summary	10
2.2	Description of the test case	10
2.3	Geometry	10
2.4	Mesh	11
2.5	Boundary conditions	11
2.6	Reference solution	12
2.7	Results	12
2.8	Conclusions	12
3	Elliptical bump on beach.: bosse_elliptique	15
3.1	Summary	15
3.2	Description of the test case	15
3.2.1	Geometry	15
3.2.2	Mesh	16
3.2.3	Boundary conditions	16
3.3	Reference solution	17
3.4	Results	17
3.5	Conclusions	17

4	Monochromatic swell breaking on beach.	20
4.1	Summary	20
4.2	Description of the test case	20
4.2.1	Geometry	20
4.2.2	Mesh	20
4.2.3	Boundary conditions	21
4.2.4	Solver	21
4.3	Results	22
4.4	Conclusion	22
5	Breach	24
5.1	Summary	24
5.2	Description of the test case	24
5.2.1	Geometry	24
5.2.2	Mesh	24
5.2.3	Boundary conditions	24
5.2.4	Solver	25
5.3	Results	25
5.4	Conclusions	26
6	Port of Borme les Mimosas (creocean)	28
6.1	Purpose	28
6.2	Description of the problem	28
6.2.1	Geometry and mesh	28
6.2.2	Boundary conditions	28
6.3	Results	31
7	Flamanville - Agitation in the intake channel : flam	32
7.1	Purpose	32
7.2	Description of the test case	32
7.2.1	Geometry	32
7.2.2	Mesh	32
7.2.3	Boundary conditions	33
7.3	Results	33
7.4	Conclusions	33
8	Friction on sandy bottom.	36
8.1	Summary	36
8.2	Description of the test case	36
8.2.1	Formulas	36
8.2.2	Geometry	37
8.2.3	Mesh	37

8.2.4	Sediments	37
8.2.5	Boundary conditions	37
8.2.6	Solver	38
8.3	Results	38
8.4	Conclusions	38
9	Wave field around a floating body	41
9.1	Summary	41
9.2	Description of the test case	41
9.2.1	Geometry	41
9.2.2	Boundary conditions	41
9.3	Reference solution	43
9.4	Results	43
9.5	Conclusions	43
10	Schematic port of Delft:port	45
10.1	Summary	45
10.2	Description of the test case	45
10.2.1	Geometry	45
10.2.2	Mesh	45
10.2.3	Mesh	45
10.2.4	Boundary conditions	45
10.3	Reference solution	47
10.4	Results	47
10.5	Conclusions	47
11	Schematic reef: recif	49
11.1	Summary	49
11.2	Description of the test case	49
11.2.1	Geometry	49
11.2.2	Mesh size	50
11.2.3	Boundary conditions	50
11.3	Reference solution	51
11.4	Results	51
11.5	Conclusions	51
12	Reflection on rippled bottom: rides	53
12.1	Summary	53
12.2	Description of the test case	53
12.2.1	Geometry	53
12.2.2	Mesh	54

12.2.3	Boundary conditions	54
12.3	Reference solution	55
12.4	Results	55
12.5	Conclusions	55
	Bibliography	58

1. Energy loss due to wave breaking: BJ78

1.1 Purpose

The objective of this test case is to compare Artemis with the results of a physical model in a case of wave energy loss due to breaking waves. The experimentation took place at Delft University of Technology [1] on a 21m x 80cm model. The objective is to validate the modeling of the dissipation due to breaking waves (Battjes and Janssen approach for random swell). The results obtained with Artemis are in good agreement with the experimental results.

1.2 Description of the test case

The modeled case and its bathymetry can be visualized on figure 1. The water height is 0.616 m at the channel entrance. The surge is taken into account (Battjes and Janssen approach) but there is no dissipation by friction on the bottom.

1.2.1 Geometry

The modeled channel is a 21 m long and 0.8 m wide rectangle. The bathymetry is set at $z = -0.616\text{m}$ at the channel entrance, then several ramps are applied:

$$\begin{aligned}x < L_1 \quad & z = -0.616 \\L_1 \leq x \leq L_1 + L_2 \quad & z = 0.05(x - L_1) - 0.616 \\L_1 + L_2 < x < L_1 + L_2 + L_3 \quad & z = -0.025(x - L_1 - L_2) - 0.116 \\L_1 + L_2 + L_3 \leq x \quad & z = 0.05(x - L_1 - L_2 - L_3) - 0.226\end{aligned}$$

1.2.2 Mesh

The mesh is a set mesh comprising 1394 triangular elements. The nodes are spaced in x and y by about 16 cm.

1.2.3 Boundary conditions

Incidental swell:

- Peak period= 1.887 s
- Significant wave height : 0.202 m
- Min and Max period of the spectrum: [0.75 s ; 8 s]

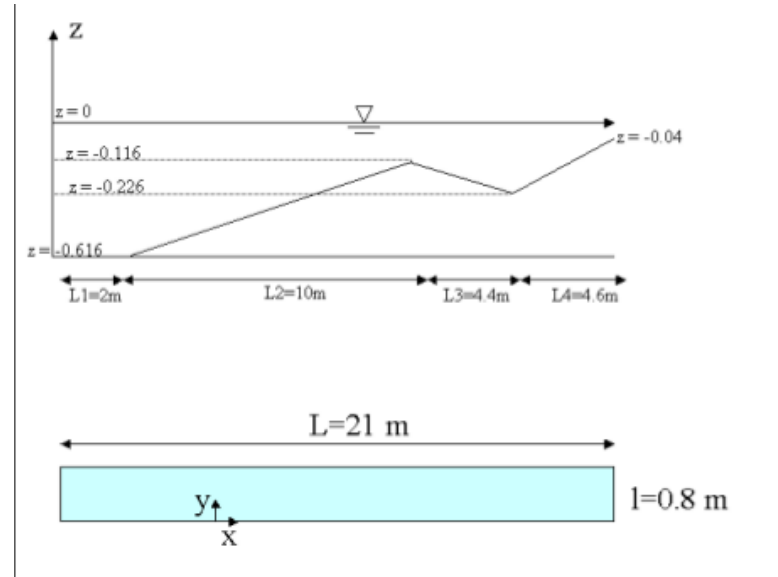


Figure 1.1: Configuration.

- JONSWAP spectrum parameter: gamma=3.3
- Propagation direction : 0° .
- Direction of exit: 0° .
- Phase (ALFAP): zero on the whole border

Walls :

- Reflection coefficient = 1.
- Phase shift : 0° .
- Angle of attack: 90° .

Output :

- Angle of attack of the outgoing waves: 0° .

1.3 Reference solution

The experimental results obtained in [2] constitute the reference values. The criterion for comparison is the energetic water height along the channel. This water height is related to the significant head by the formula :

$$H_s = \sqrt{2}H_e$$

The measured and calculated free surface elevations are therefore compared.

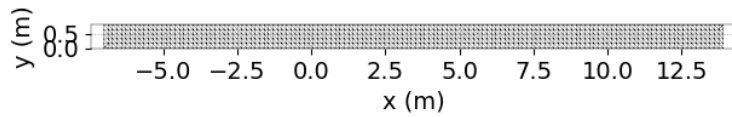


Figure 1.2: Mesh.



Figure 1.3: Boundary conditions.

1.4 Results

The results are presented in figure 1.4.

The Artemis results correlate well with the experiment. The energy loss due to the is well predicted in the case of a random swell. The code gives satisfaction in terms of in terms of intensity and spatial distribution of this dissipation, the use of the formula of Battjes and Janssen's formula is a good way to model the dissipation related to the breaking resulting from bathymetric variations.

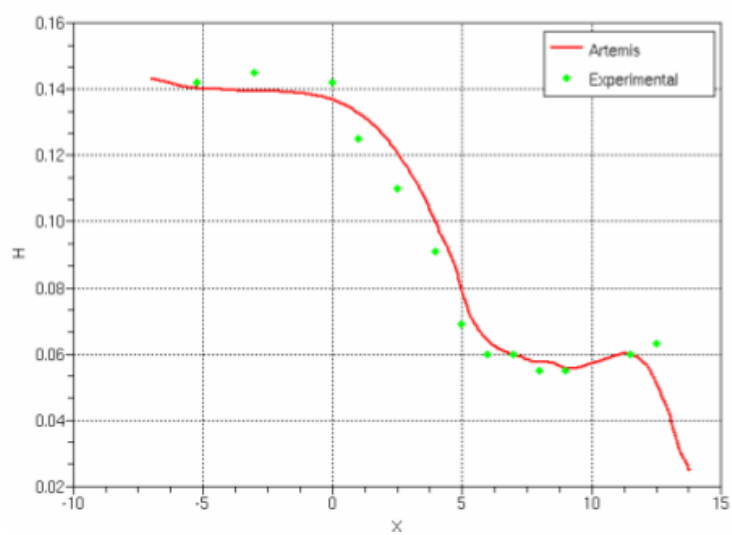


Figure 1.4: Energetic wave height (m) as a function of the position in the channel (m). Red curve: ARTEMIS, green points: Battjes and Janssen experiment [2].

2. Transformation of a wave on a circular bump: bosse

2.1 Summary

The objective of this test case is to analyze the predictions of Artemis in the case of a bathymetry with a bump of significant height. This case highlights the interest of taking into account the slope and curvature terms in the Berkhoff equation (extended diffraction-refraction equation refraction equation, option *RAPIDLY VARYING TOPOGRAPHY*). We compare Artemis to experimental results [19].

We consider the case of a basin with an analytical bathymetry, defining a circular bump. This case was defined by [19], then taken up by [6] and [14]. It allows to study the reflection-diffraction phenomenon for a wave propagating over a highly variable bottom, with effects in the 2 directions of the free surface plane. The interest of this case, in addition to give a reference to validate Artemis, is that it is a case that is quite discriminating between predictions of the Berkhoff equation alone and predictions of the extended Berkhoff equation. The results are quite satisfactory.

2.2 Description of the test case

The general configuration is described in Figure 2.1, which presents the bathymetry and dimensions of the dimensions of the channel. The detailed bathymetry can be found in 2.3
For the numerical model, we set $R=1\text{m}$. We use the geometric ratios proposed by [19]. In particular :

- $b/H = 0.807$
- $b/R = 0.4$
- $kH = 3$

where k is the wave number of the incident wave.

The breaking is not taken into account, no friction on the bottom is taken into account either.

2.3 Geometry

The modeled basin is a rectangle of 12 m long and 20 m wide.

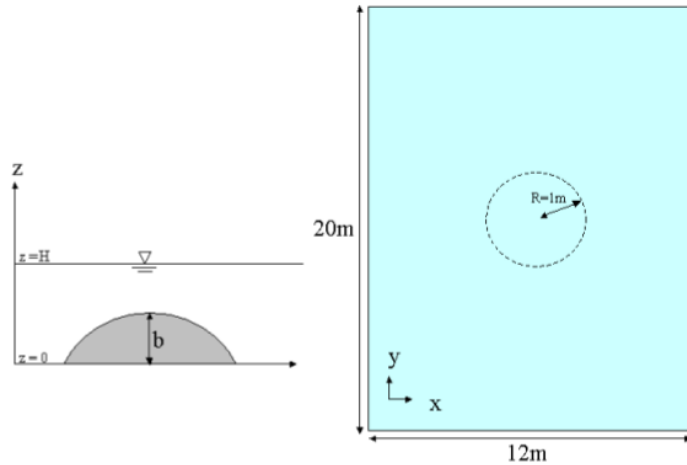


Figure 2.1: Configuration of the problem

The bathymetry is set at $z=0$ everywhere in the basin, except at the hump. The hump is centered on the point $x_c = 6m$ and $y_c = 10m$:

$$d = \sqrt{(x - x_c)^2 + (y - y_c)^2} < R \quad \Rightarrow z = b(1 - (\frac{d}{R})^2)$$

2.4 Mesh

The mesh used is an adjusted mesh generated by Janet. It has 1 200 000 elements triangular elements. The nodes are regularly spaced by 2 cm on the abscissa and ordinate.

2.5 Boundary conditions

The boundary conditions of the domain are presented in Figure 2.2.

Incidental swell:

- Period 0.633s
- Wave height: 0.01 m-
- Propagation direction: 0° .
- Exit direction: 0° .
- Phase (ALFAP) : 0° on the whole liquid boundary

Wall:

- Reflection coefficient = 1.
- Phase shift : 0°
- Angle of attack: 0°

Free exit:

- Angle of attack of the outgoing waves: 0° .

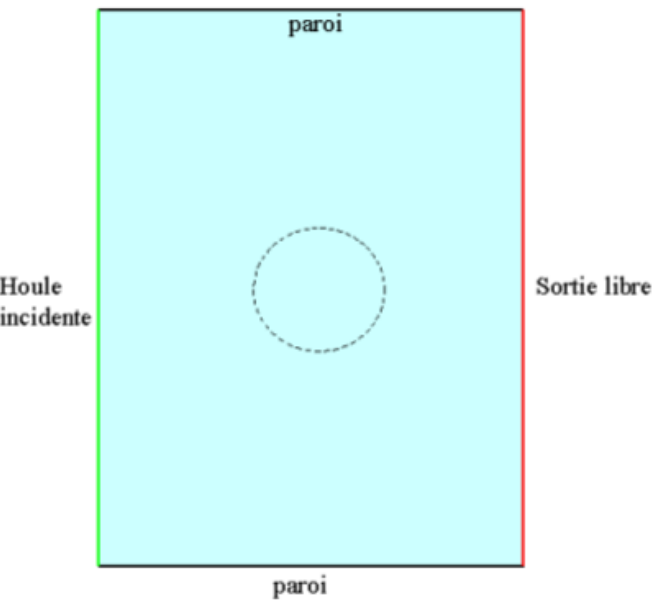


Figure 2.2: Configuration of the problem

2.6 Reference solution

The experimental results proposed in [6] are the reference data. They are wave heights measured in some planes. They are presented in the form of normalized wave height :

$$\frac{H}{H_{\text{incident}}}$$

with H_{incident} the incident wave height.

We have chosen the plane noted "a" by the authors (see Figure 2.3) because of its character discriminant between the Berkhoff equation and the extended Berkhoff equation.

2.7 Results

The results obtained with Artemis in the "a" plane and the experimental reference are presented below in figure 4.

We give the results with and without taking into account the effects of slope and curvature. We note that in the case studied, the use of the extended Berkhoff equation allows a better estimation of the experimental results. This is particularly true for the prediction of the extreme height.

The comparison is satisfactory. Taking into account the second order bathymetric effects has allowed to better estimate the effects has allowed to better estimate the water level amplification.

2.8 Conclusions

This test case allows to validate Artemis on a wave tank test. The numerical results are in general in good agreement with the experimental ones, when using the *RAPIDLY VARYING TOPOGRAPHY* option. This option allow to take into account the effects of slope and curvature in the Berkhoff equation.

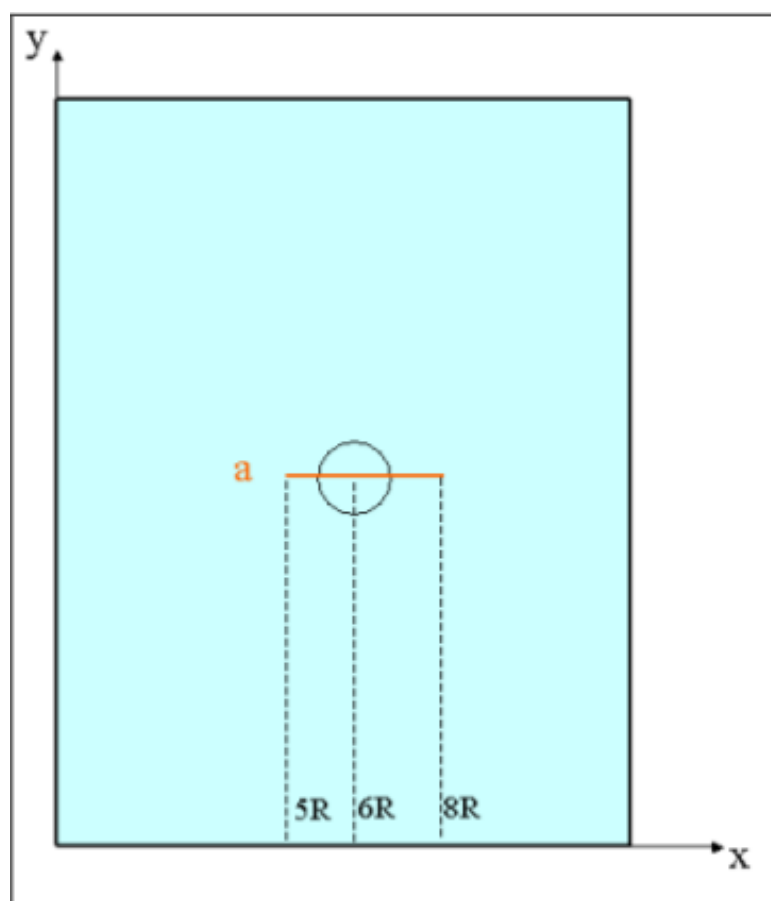


Figure 2.3: Definition of the plan “a”

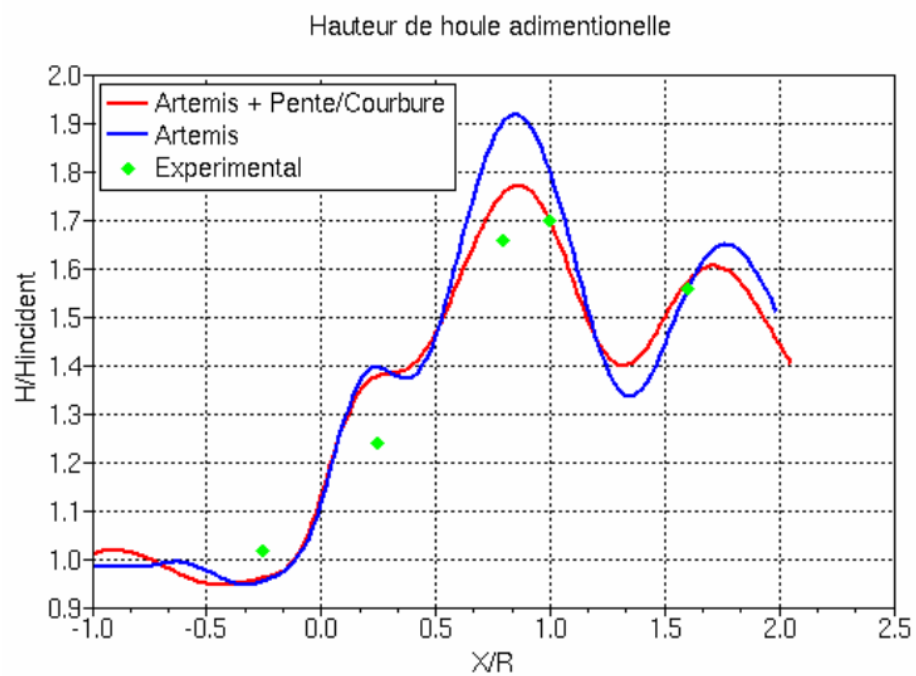


Figure 2.4: Water height in plane a. Comparison between the experiment (green points) and 2 ARTEMIS calculations: in blue without taking into account slope and curvature effects, in red with

3. Elliptical bump on beach.: bosse_elliptique

3.1 Summary

The objective of this test case is to analyze the behavior of Artemis during the transformation of the swell over a bump on a beach. When we consider exclusively the beach, the transformation of the swell is only due to refraction. In presence of the bump, the coupling between refraction and diffraction appears. The refraction methods, applied in this case, lead to a convergence of the swell behind the hump, associated with a concentration of energy. In reality, the energy of the swell is dispersed, which is mainly due to diffraction in the lateral direction.

The results are compared with experimental results presented by Berkhoff [11]. They verify that the coupling between refraction and diffraction is well taken into account by the Artemis code.

3.2 Description of the test case

The modeled case represents the one realized in [11], i.e. a bump, on a beach on the side opposite to the generation of the swell. The angle between the beach and the swell direction is 20° . The side edges are solid walls. The slope and curvature terms are taken into account in the Berkhoff equation (extended diffraction-refraction equation, option *RAPIDLY VARYING TOPOGRAPHY*).

3.2.1 Geometry

Domain

- Size domain: 30 m x 35 m
- Max depth: 0.45m
- Beach slope: 1/50

Elliptical Bump

- Large axis: 8m
- Small axis: 6m
- Max height: 0.2m

3.2.2 Mesh

- Triangular elements: 49083
- Mesh size: 20 cm
- Nodes: 24842
- Meshes per wavelength: 7.5 (for $h = 0.45$ m)

3.2.3 Boundary conditions

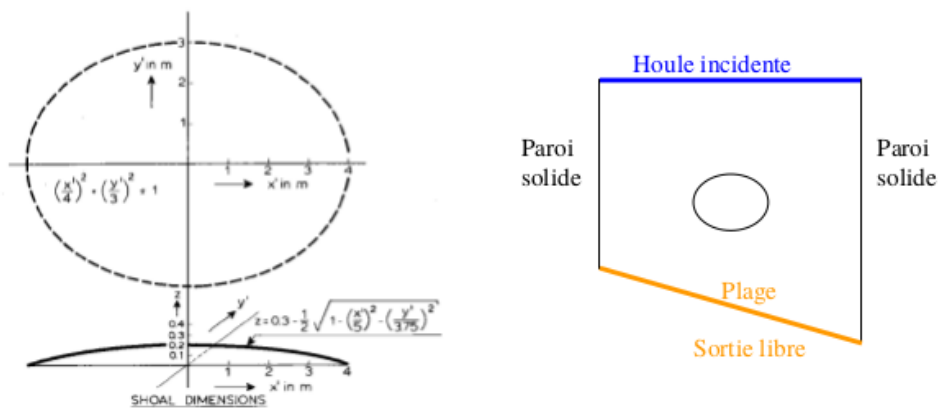


Figure 3.1: Dimensions and Boundary conditions

Incidental swell:

- Period: 1 s
- Wave height : 0.0464 m
- Zero phase on the whole boundary : ALFAP=0
- Direction of propagation: 90°.

Solid walls:

- Reflection coefficient: 0
- Phase shift : 0°
- Angle of attack : 90°

Liquid wall:

- Reflection coefficient: 0
- Phase shift: 0°
- Angle of attack: 20°

3.3 Reference solution

The experimental results obtained in [11] constitute the reference values, divided into 8 sections. We compare the wave heights obtained numerically and experimentally by presenting the amplification coefficient, defined by the following formula:

$$\frac{H(x,y)}{H_{\text{incident}}}$$

3.4 Results

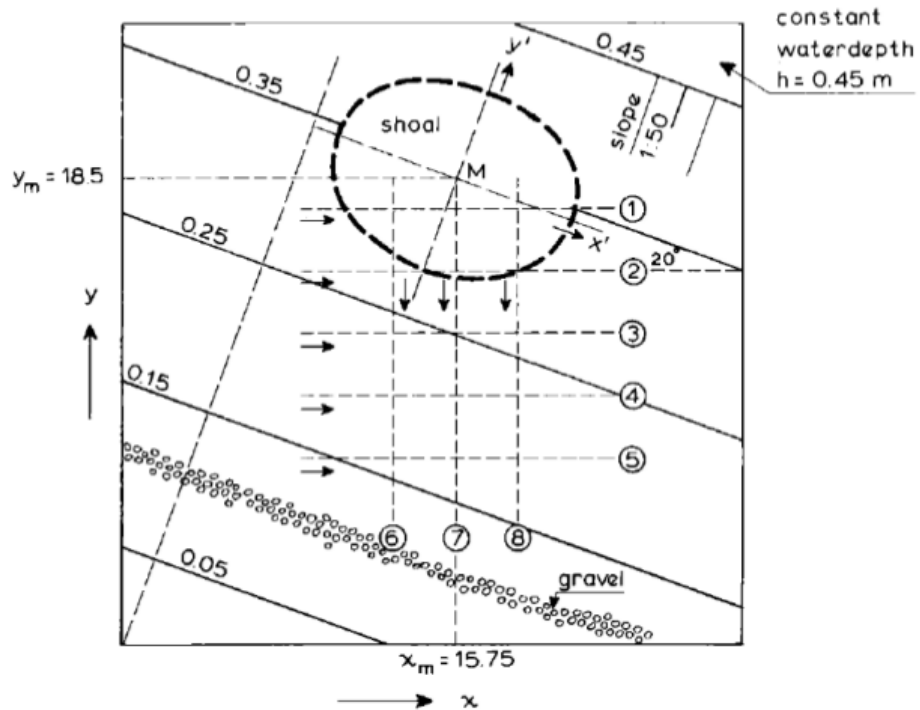


Figure 3.2: definition of sections

The wave amplitudes obtained with the solver 3 (figure 3.3) are compared to those presented by Berkhoff [11]. The measurements were taken along different sections parallel to the x and y axes, represented on the diagram below (figure 3.2).

The comparison (figure 3.4) between the results obtained by Artemis and those obtained in [11] shows good correspondences. We can clearly see the effect of the bump: a maximum amplification of 227%. Experimentally, this maximum is 221%. This highlights that Artemis takes into account the refraction-diffraction interactions.

3.5 Conclusions

This test case compares the results produced by Artemis with experimental results on physical model. It allows to validate the modeling of the combined effects of refraction and diffraction.

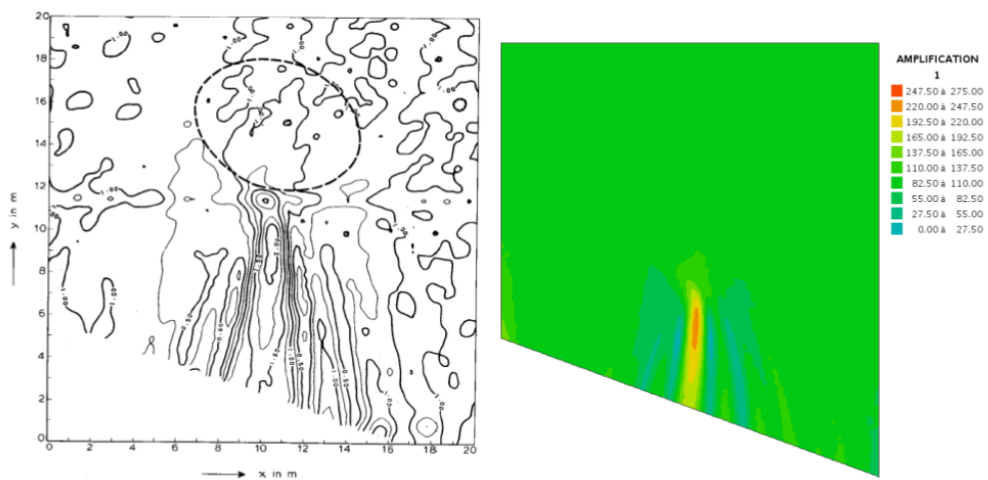


Figure 3.3: amplification coefficient of wave height with Berkhoff (on left) and artemis (on right)

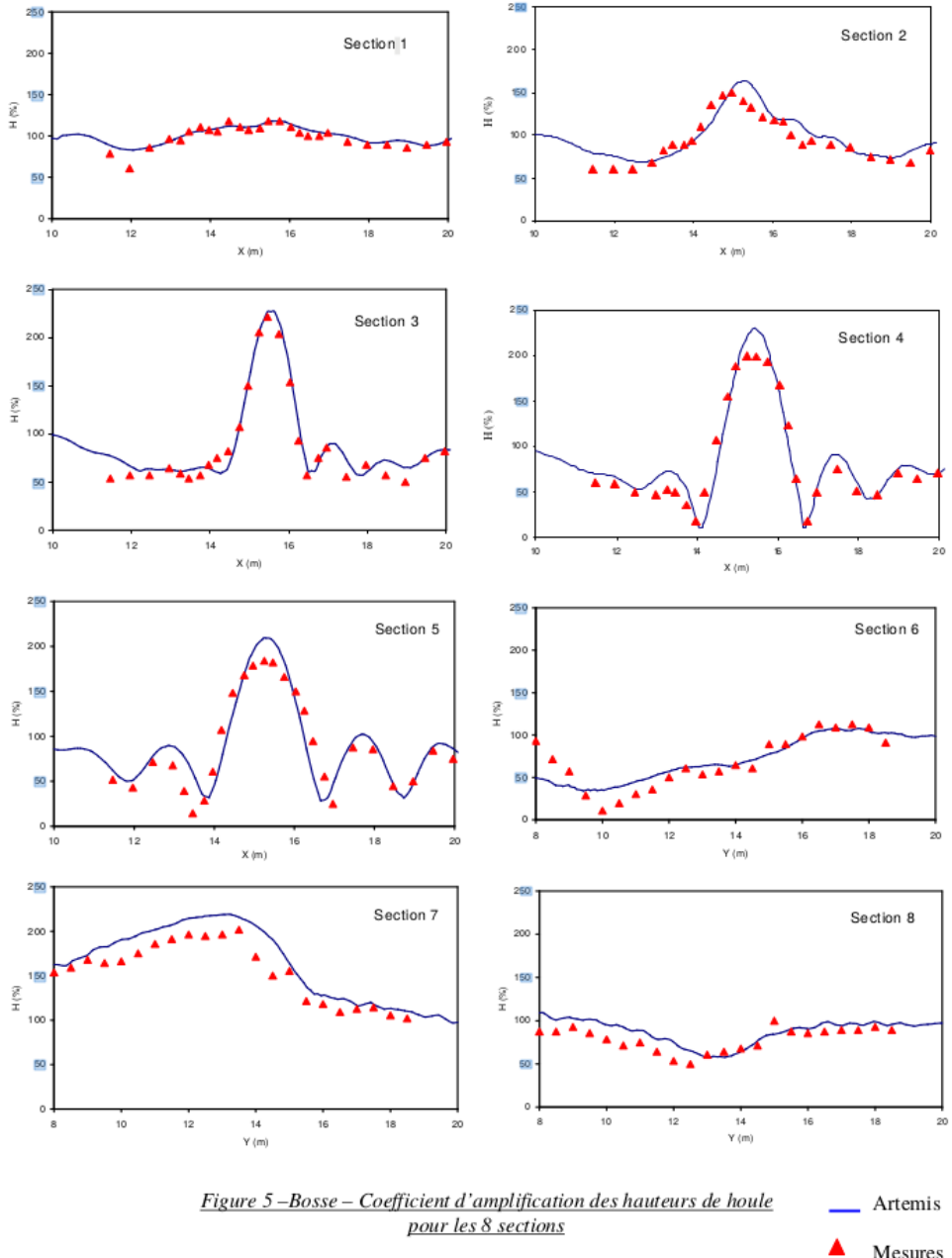


Figure 3.4: amplification coefficients of wave height for the 8 sections.

4. Monochromatic swell breaking on beach.

4.1 Summary

The aim of this test case is to analyze the behavior of Artemis during wave breaking on a beach with a constant gentle slope. It also enables us to test the two breaking model introduced in Artemis.

The results are compared with experimental results obtained on a physical model by Delft Hydraulics Laboratory [16]. They enable us to verify that the Artemis code takes well into account wave breaking

4.2 Description of the test case

The modeled case is the one described in [16], i.e. a beach on the opposite side to the swell generation. Two breaking formulas are compared. In the first case we use the formula of Battjes & Janssen [2] and in the second case we use that of Dally et al [7]. For the latter case we set $K=0.25$ and $\Gamma = 0.4$. These choices were based on the values proposed by Dally et al [7], and after tests carried out on the Artemis code for several values of K and Γ .

4.2.1 Geometry

Domain: 42.5m x 1m

maximum depth: 0.7m

beach slope: 1/40

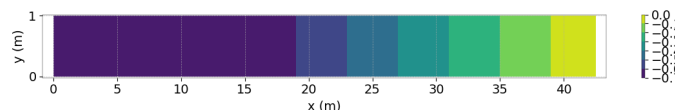


Figure 4.1: Bathymetry of the case

4.2.2 Mesh

Number of triangular elements: 1421

size of mesh: 40 cm (inlet) 10 cm (outlet)

Nodes: 863

number of mesh per wavelength: 11.7 (for $h=0.7m$)

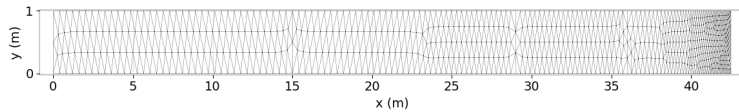


Figure 4.2: Mesh of the case

4.2.3 Boundary conditions

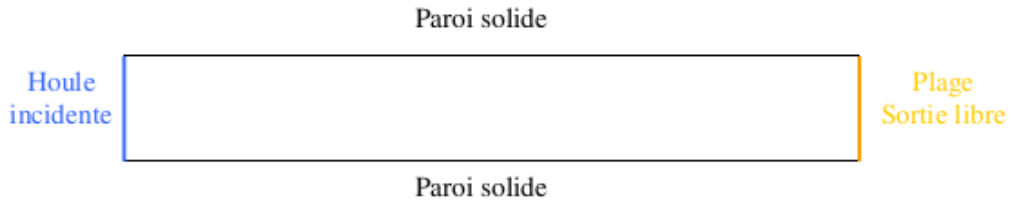


Figure 4.3: Boundary Conditions

Incident swell:

- Period: 1.79 s
- Swell height: 0.145 m
- Phase (ALFAP): 0 on all the boundary
- propagation direction: 0°

Solid wall:

- Reflection Coefficient: 1
- Dephasing: 0
- attack angle: 0°

liquid wall (beach):

- Reflection Coefficient: 0
- Dephasing: 0
- attack angle: 0°

4.2.4 solver

For both cases, the direct solver (solver = 8) was used with accuracy of 10^{-4} . Calculation time is less than 1 second. For the dissipation coefficient calculation, the relaxation coefficient between two sub iterations is 0.25.

4.3 Results

The experimental results obtained in [16] are the reference values. The points are on a section for x from 34 to 42m and $y = 0.5\text{m}$. We compare wave height experimentally and numerically. The wave height of swell obtained for the two models are compared on figures 4.4 and 4.5, the breaking rate on figures 4.6 and 4.7. Figure 4.8 compares the result obtained with Artemis with the 2 models and the experimental results. The measurements used to make the Figure, have been approximated with the reading of an old Figure A comparison (Figure 4.8) between the results obtained by Artemis and those obtained in [] shows good correspondence. It shows that Artemis has adequately taken into account breaking phenomena. Nevertheless, the results produced by Artemis are overestimated compared to the measurements. However, Dally's formula seems to slightly less overestimate.

There is a simple explanation for the discrepancy between numerical and experimental results. The shallow slope leads to a spilling breaking which means that the dissipation occurs on a long distance and not in a restricted area. In the case of a monochromatic swell the breaking rate is 0 or 1 which gives breaking or not at all. This binary description is not suitable to that type of breaking, which explain the overestimation in the surfing area. The differences will be less important for a random swell.

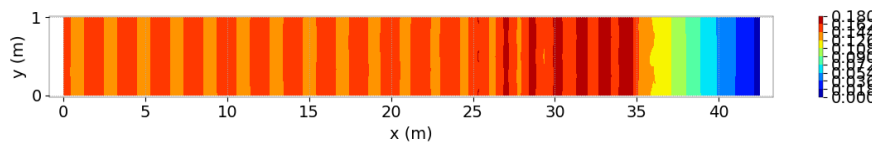


Figure 4.4: Wave height with Dally model

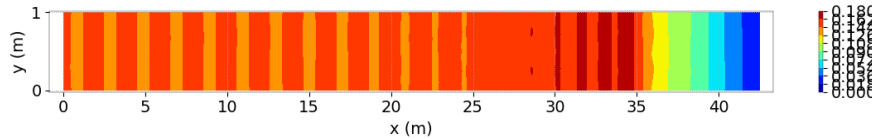


Figure 4.5: Wave height with Janssen model

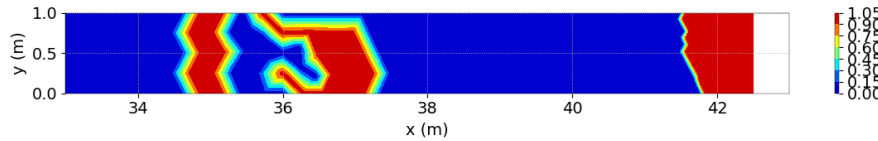


Figure 4.6: Breaking rate with Dally model

4.4 Conclusion

This test case compares the results produced by Artemis with experimental results on a physical model. It validates Artemis' ability to take into account wave breaking for a monochromatic swell. However, this type of swell is not suitable for modeling of all breaking modes, especially

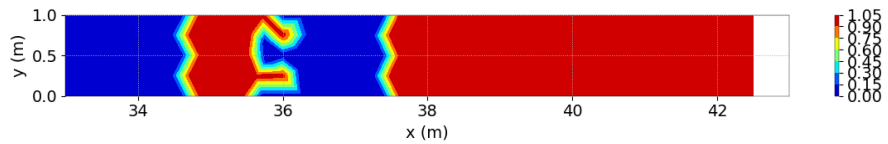


Figure 4.7: breaking rate with Janssen model

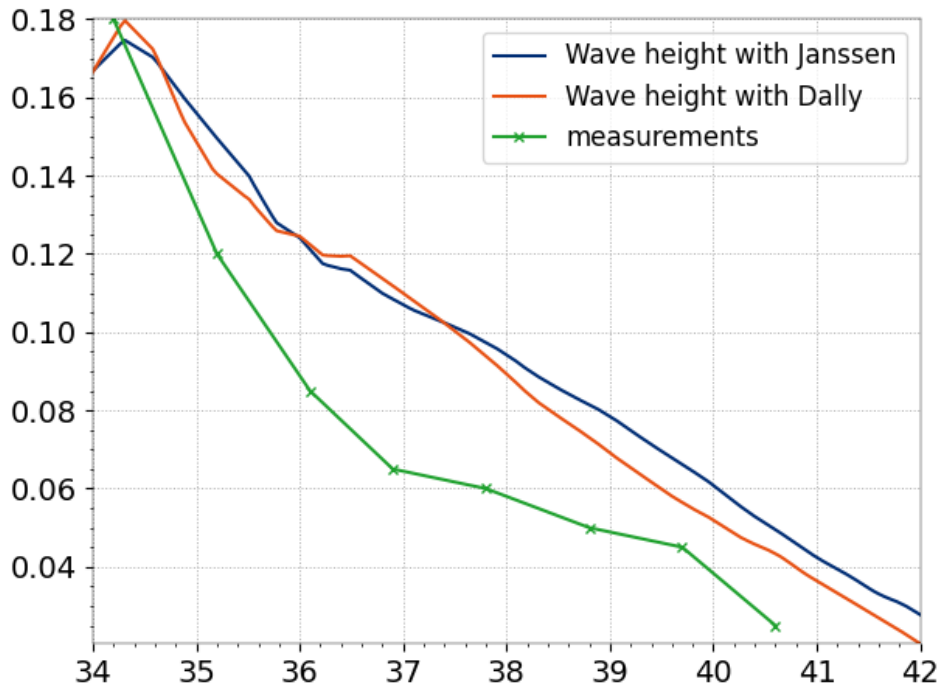


Figure 4.8: Comparison of wave height with measurements on a profile

for sliding waves. It is therefore recommended to use Artemis with a random swell, especially when breaking plays an important role in wave propagation.

5. Breach

5.1 Summary

The aim of this test case is to compare the results produced by Artemis with experimental results on a known application: the diffraction of a swell entering a harbor through a gap twice its wavelength. The results are compared with those given by the Shore Protection Manual of the Coastal Engineering Research Center, USA (CERC, [5], page 2-93).

5.2 Description of the test case

The modelled case represents a narrow entrance to a square port with a constant flat bottom.

5.2.1 Geometry

Port Entrance: 550m

Domain: 1830mx1830m

Water depth: 64 m

5.2.2 Mesh

Number of triangular elements: 14304

Nodes: 7313

Mesh per wavelength: 14

5.2.3 Boundary conditions

Incident swell:

- Period: 14 s
- Wave height: 1 m
- Phase (ALFAP): 0 on all the boundary
- Propagation direction: 0°

Solid wall:

- Reflection coefficient: 1
- Dephasing: 0

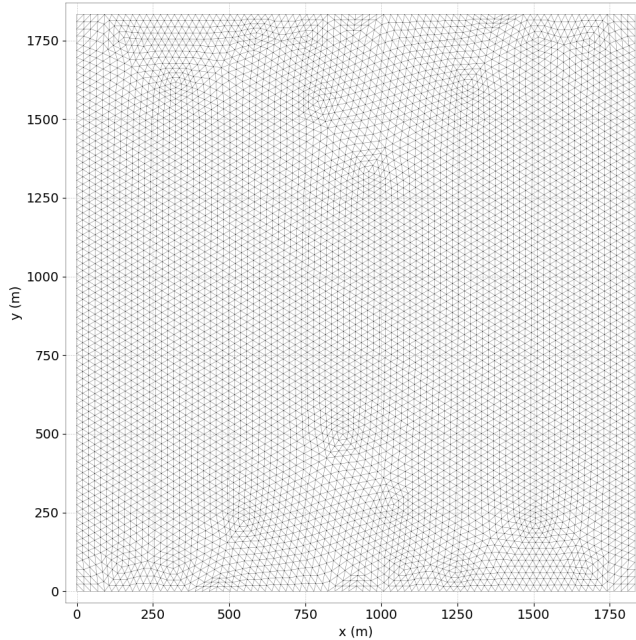


Figure 5.1: Mesh of the case

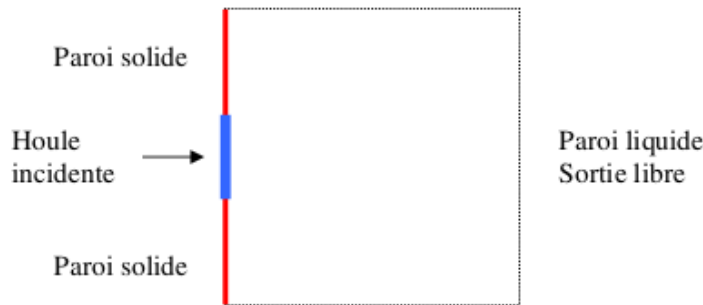


Figure 5.2: Boundary Conditions

- Attack angle: 0°

Paroi liquide :

- Attack angle: 0°

5.2.4 Solver

Two solver have been tested with a precision of 10^{-4}

- Direct solver (solver=8) time of calculation less than 1s.
- Conjugate gradient on a normal equation (solver=3) time of calculation of 2s.

5.3 Results

The experimental results obtained in [4] constitute the reference values, distributed over a section shown in section shown in Fig 5.4. A comparison is made between the wave heights

obtained numerically and experimentally.

The results obtained by Artemis (Solver 8) are shown figure 5.3, the ones obtained by the CERC is on Figure 5.4 and the comparison between both are shown in Figure 5.5.

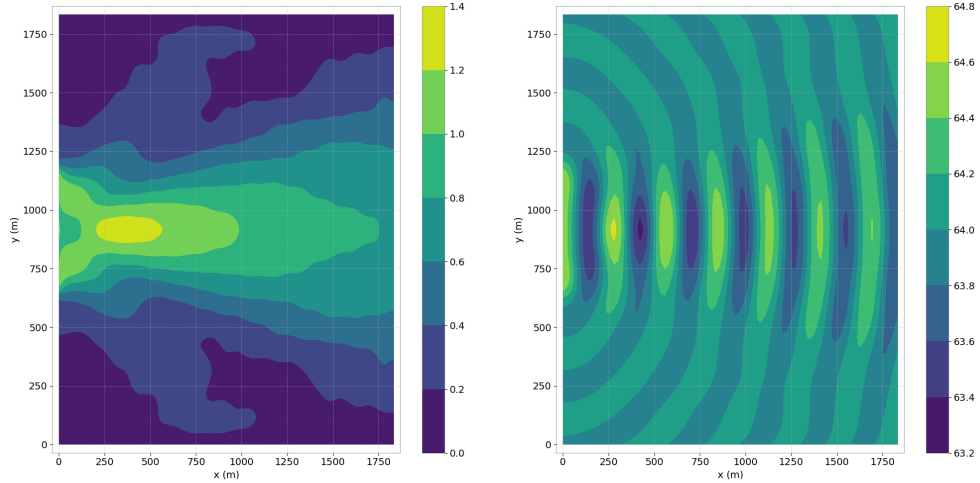


Figure 5.3: Breach: Wave height on left and free surface on right

5.4 Conclusions

This test case compares results acquired with Artemis with experimental results. It validates the wave diffraction model. The agreement between numerical predictions and experiment is satisfactory.

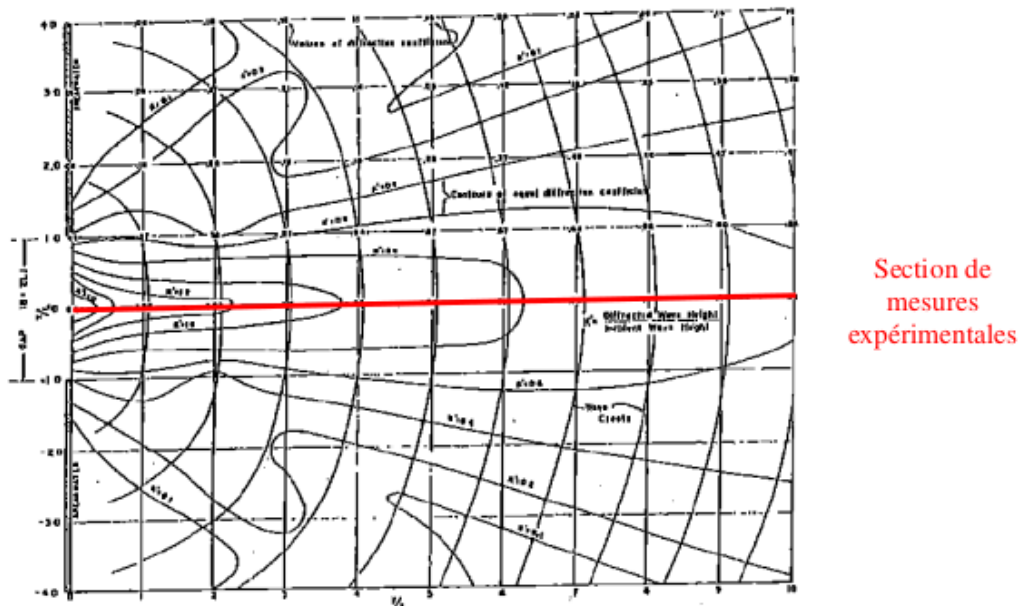


Figure 5.4: Breach:

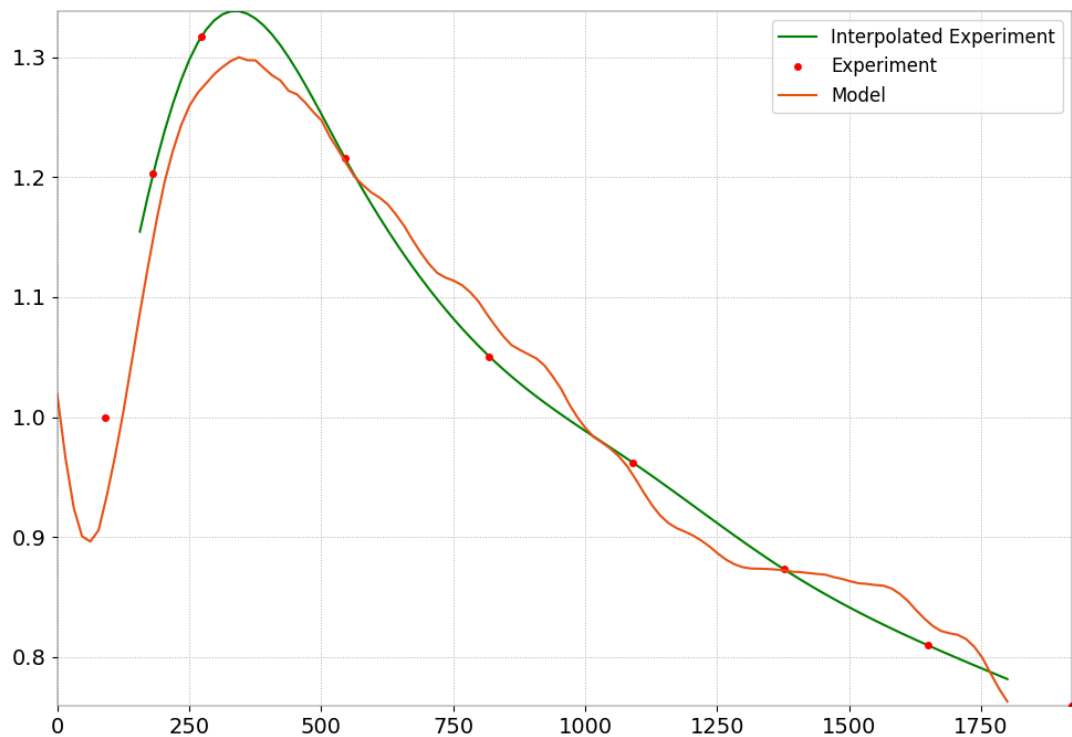


Figure 5.5: Breach: Comparison of wave height between measurements and Artemis

6. Port of Borme les Mimosas (creocean)

6.1 Purpose

This Artemis case describes the analysis of the harbor agitation in the port of Borme les Mimosas. It gives an example of the use of the code in a concrete case: choice of different reflection coefficients of reflection, parallel calculation, etc...

6.2 Description of the problem

6.2.1 Geometry and mesh

The domain is equally delimited by the solid and liquid walls. Several assumptions are applied for the liquid boundary conditions to the north, as well as for the solid walls. We will detail them in 2.3. The bathymetry can be visualized in Figure 6.1. The initial coastline of the free surface is 0.5 m.

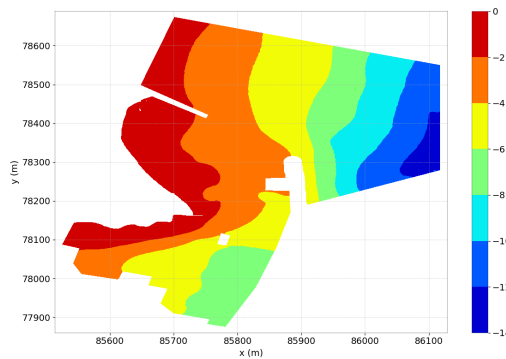


Figure 6.1: Geometry.

The mesh consists of 62261 triangle elements and 31645 nodes. The size of a mesh is 3m. The mesh can be visualized on figure 6.2.

6.2.2 Boundary conditions

Incident wave: Wave 1 :

- Peak period = 8 s

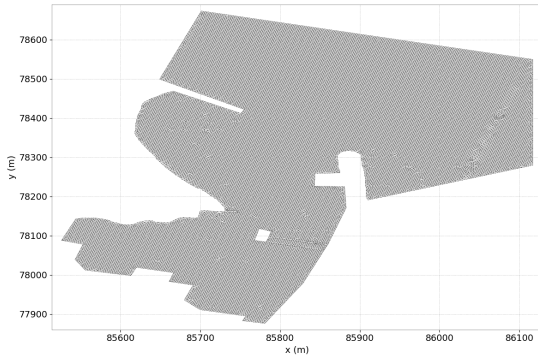


Figure 6.2: Mesh.

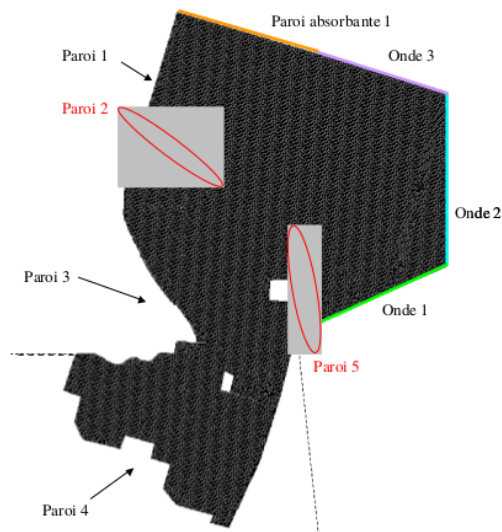


Figure 6.3: Bound.

- Max and Min period : 12 s and 6 s.
- Spectrum parameter: gamma = 2.
- Wave height : 2 m
- Direction of propagation $\theta = 180^\circ$
- Exit direction : 63° .

Wave 2:

- Peak period = 8 s
- Max and Min period : 12 s and 6 s.
- Spectrum parameter : gamma = 2.
- Wave height : 2 m
- Direction of propagation : $\theta = 180^\circ$

- Exit direction : 0° .

Wave 3:

- Peak period = 8 s
- Max and Min period : 12 s and 6 s.
- Spectrum parameter : gamma = 2.
- Wave height : 2 m
- Direction of propagation : $\theta = 180^\circ$.
- Exit direction : 73° .

For these three boundaries, the phase is computed incrementally on the boundary from a reference point, which we will denote A :

$$\Phi_I = \sum_{P=A}^{I-1} k(P) \cos(\Theta)(x_{P+1} - x_P) \quad (6.1)$$

Where $k(P)$ is the wave number at the boundary point P. This phase, converted to degrees, is provided to the code in the ALFAP table. Walls : Absorbing wall 1 :

- Reflection coefficient = 0.
- Phase shift : 0° .
- Angle of attack: 0° .

Wall 1 :

- Reflection coefficient = 0.05
- Phase shift : 0° .
- Angle of attack : 0° .

Wall 2 :

- Reflection coefficient = 0.15
- Phase shift : 0° .
- Angle of attack : 45° .

Wall 3 :

- Reflection coefficient = 0.05
- Phase shift : 0° .
- Angle of attack : 0° .

Wall 4 (+ island):

- Reflection coefficient = 1.
- Phase shift : 0° .
- Angle of attack : 0° .

Wall 5 :

- Reflection coefficient = 0.15
- Phase shift : 0° .
- Angle of attack : 0° .

6.3 Results

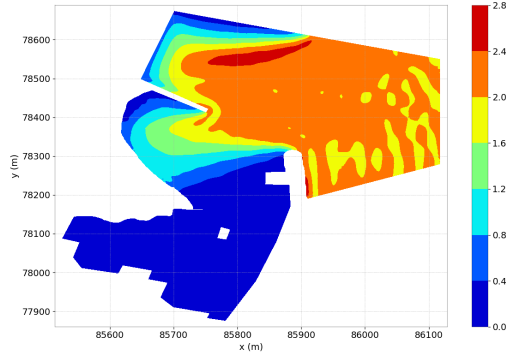


Figure 6.4: Wave Height.

Figure 4 shows the wave heights calculated by ARTEMIS using an incremental phase calculation. The other requested graphical outputs (not shown here) are wave incidence, bathymetry and breaking ratio.

The goal is to obtain a domain that is not very sensitive to the choice of the phase because this data is generally less well known than the wave height or the period. Our recommendation is to choose liquid boundaries with fairly homogeneous bathymetries, avoiding imposing the incident swell too close to the harbor as it is the case in example. Although it is preferable to ensure good physical consistency of the input data.

This example gives a concrete case of the use of Artemis, with random swell monodirectional swell. The choice of the reflection coefficients as well as the angles of attack of the are interesting for the user. Moreover, we find in this test case examples for the treatment of the phase.

7. Flamanville - Agitation in the intake channel : flam

7.1 Purpose

This Artemis case describes the wave analysis in the intake channel of the Flamanville power plant. It gives an example of the use of the code in a concrete case: boundary conditions read from a TOMAWAC file, different reflection coefficients, parallel calculation

7.2 Description of the test case

7.2.1 Geometry

The domain is largely limited by the solid walls of the channel. The only liquid boundary is constituted by the incident swell at the entrance of the channel. The bathymetry can be visualized on figure 7.1. The initial coastline of the free surface is 12.71 m.

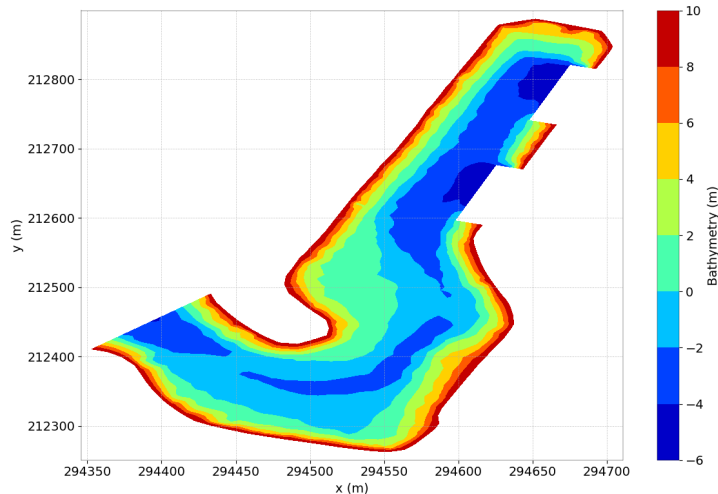


Figure 7.1: Bathymetry.

7.2.2 Mesh

The mesh consists of 5258 triangle elements and 2781 nodes. The size of a mesh is 7m. The mesh can be visualized on figure 7.2.

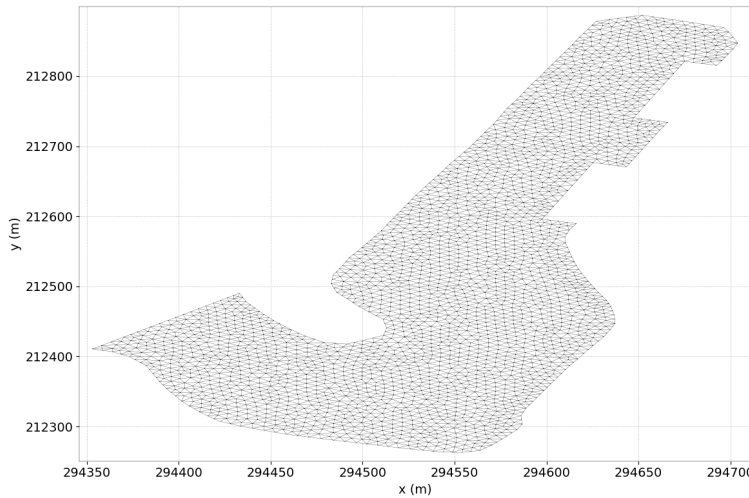


Figure 7.2: Mesh.

7.2.3 Boundary conditions

The incident swell is partly read in a TOMAWAC file. The significant heights and propagation directions are retrieved. A JONSWAP spectrum is then applied.

- Peak period: 13 s
- Max and Min period: 26 s and 6 s.
- Spectrum parameter: gamma = 3.
- Phase (ALFAP): 0°.

Wall 1:

- Reflection coefficient = 0.5
- Phase shift : 0°
- Angle of attack : 0°

Wall 2 :

- Reflection coefficient = 1.
- Phase shift : 0°
- Angle of attack : 0°

7.3 Results

The requested graphical outputs are the significant wave height, the phase, the bathymetry, breaking rate, phase velocity.

7.4 Conclusions

This example of use gives a concrete case of the use of Artemis, with random swell known in amplitude and direction. The reading of the boundary conditions, from a TOMAWAC file, gives an interesting example to the user.

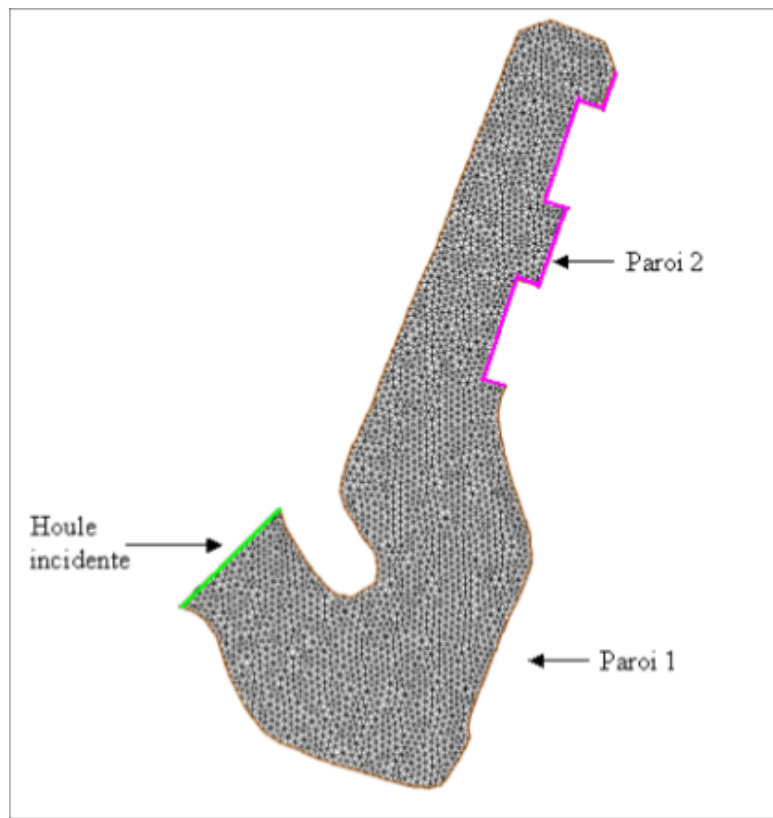


Figure 7.3: Boundary conditions

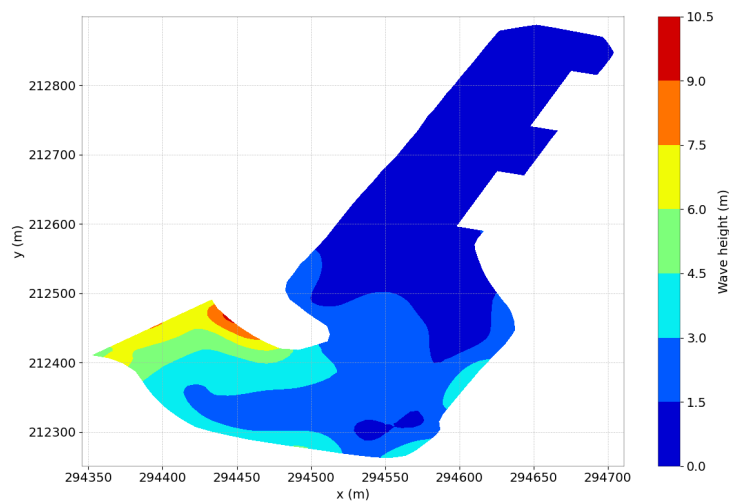


Figure 7.4: Wave Height.

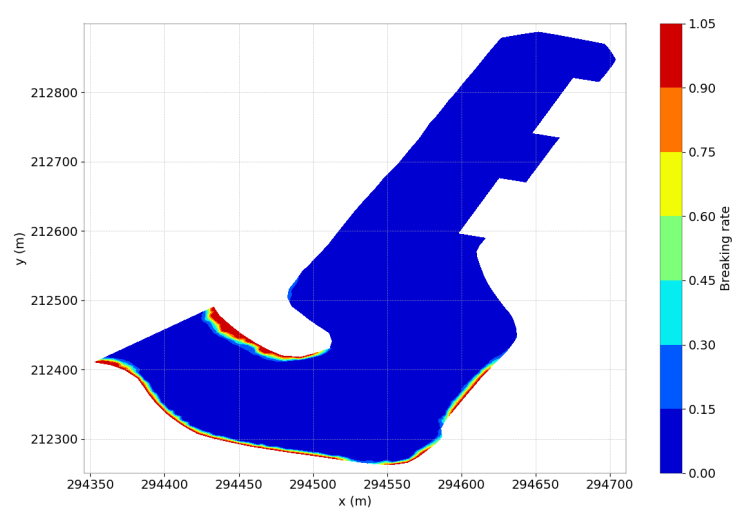


Figure 7.5: Breaking rate.

8. Friction on sandy bottom.

8.1 Summary

The aim of this test case is to analyze the behavior of Artemis when damping swell height due to bottom friction forces. The results are compared with experimental results obtained on a physical model by Inman & Bowen [10]. They are used to verify that the Artemis code correctly take into account bottom friction.

8.2 description of the test case

The case modeled is the one described in [10]. Wave damping is simulated using the bottom friction calculated by Artemis on the basis of sediment characteristics (grain diameters d_{50} and d_{90}). Artemis automatically calculates the overall roughness which takes into account both skin friction and shape friction.

This roughness, together with the type of flow (laminar or turbulent), then determines the friction factor used in formulating the dissipation coefficient. The friction formulation used here is the one of Putnam & Johnson [18]. The results considering only skin roughness are also presented.

8.2.1 Formulas

The general roughness formula used is as follows:

$$k = k_p + k_f$$

k_p is the skin roughness, which depends on the size of grain and on the type of flow:

$$\begin{aligned} k_p &= 3d_{90} && \text{for } \Theta < 1 \\ k_p &= 3\Theta d_{90} && \text{for } \Theta \geq 1 \end{aligned} \tag{8.1}$$

Θ is the Shields mobility parameter, relative to the flow, which expresses the ratio between the force resulting from the shear stress on the grain and the immersed weight of the grain calculated as a function of d_{50} (Van Rijn [13]).

k_f represents the shape roughness, i.e. the roughness due to the formation of wrinkles, we use the formula proposed by Van Rijn [13]:

$$k_f = 20\Gamma_r \Delta_r \left(\frac{\Delta_r}{\lambda_r} \right)$$

- Δ_r Wrinkles height
- λ_r Wrinkles wavelength
- Γ_r Wrinkle presence factor (equal to 1 for wrinkles alone, equal to 0.7 for wrinkles superposed on sand waves). Here, it is equal to 0.7.

Once the roughness has been calculated, we can obtain the friction factor f_w , whose formula depends on the type of flow. For rough turbulent flow, we use the expression given by Van Rijn [13]. Finally, we get the expression for the shear stress due to the Putnam & Johnson formula [17].

8.2.2 Geometry

Domain: 20 m x 2 m

Water depth: 0.5 m

8.2.3 Mesh

Triangular elements: 1896

Taille des mailles: 0.13 m (longitudinal max)

Nodes: 1169

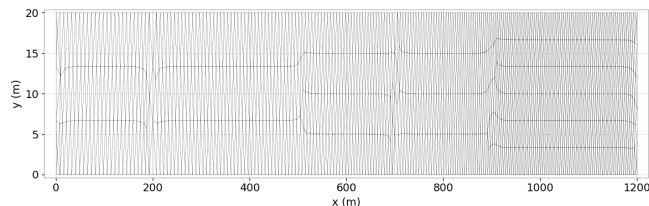


Figure 8.1: Mesh of the case

8.2.4 Sediments

Caracteristical diameters:

- $D_{50} = 0.2 \text{ mm}$
- $D_{90} = 0.3 \text{ mm}$

8.2.5 Boundary conditions

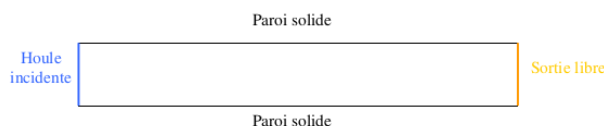


Figure 8.2: boundary conditions

Houle incidente :

- Period: 2 s
- swell height: 0.175 m
- Phase (ALFAP): 0 (on all the liquid boundary)
- Propagation direction de propagation: 0°

Solid Wall:

- Reflection Coefficient: 1
- Dephasing: 0
- Attack angle: 0°

Liquid wall:

- Reflexion coefficient: 0
- Dephasing: 0
- Attack angle: 0°

8.2.6 Solver

The direct solver (solver = 8) was used with accuracy of 10^{-4} . Calculation time is less than 1 second.

8.3 Results

The experimental results obtained in [4] constitute the reference values, distributed over a section at $y=1\text{m}$.

The measurements were taken once ripple formation and sediment transport had reached a stable state. ripple formation and sediment transport have reached a steady state. We compare the wave heights1 obtained numerically and experimentally. We also compare the ripple characteristics.

The comparison (figure 8.4) between wave height calculated by artemis and the ones obtained in [4] show good behavior. It highlights how well Artemis takes into account by Artemis of the frictional stresses exerted by the seabed and the reduction in swell height due to this friction.

In addition, Table 8.1 shows the results obtained for ripple characteristics with a friction factor $f_w = 0.17$ (calculated by Artemis). The correlation with the results of Inman & Bowen [1] is satisfactory. Artemis is therefore able to determine whether or not wrinkles are formed, and thus to deduce their characteristics.

The height and wavelength of the ripples are much greater than the size of the sediment, which explains the poor results: the height and wavelength of the ripples are much greater than the size of the sediment, which explains the poor results obtained by considering only the skin roughness.

8.4 Conclusions

This test case compares the results produced by Artemis with experimental results. It validates the inclusion of bottom friction and the calculation of ripple characteristics by Artemis.

In this case, Artemis calculates the friction factor from the size of the sediments. sediments. However, it is possible to impose it if the user wishes or if the bottom is not sandy. However, the values imposed are often taken from classic tables which generally determined for stationary flows. Here, however, the flow is oscillating because it is subject to wave action.

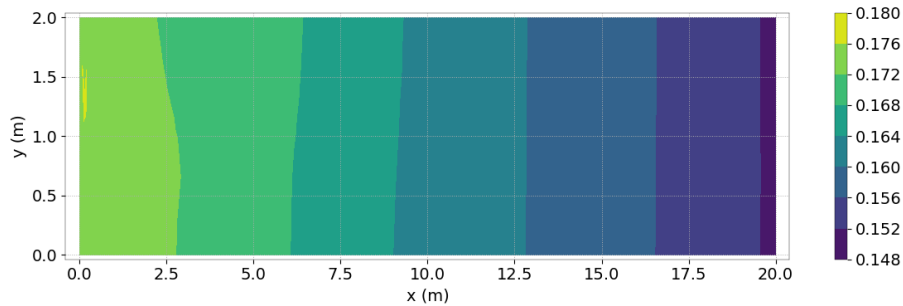


Figure 8.3: Wave height

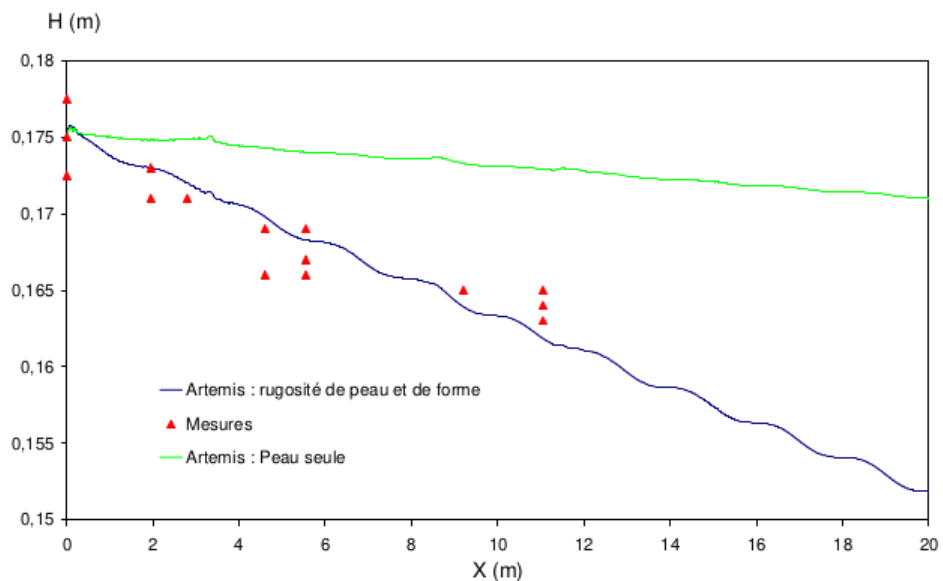


Figure 8.4: Wave height Comparison with measure

	$\Delta_r(cm)$	$\lambda_r(cm)$
Artemis	1.5	8.6
Berkhoff	1.5	10.8

Table 8.1: Height and wavelength of the ripples

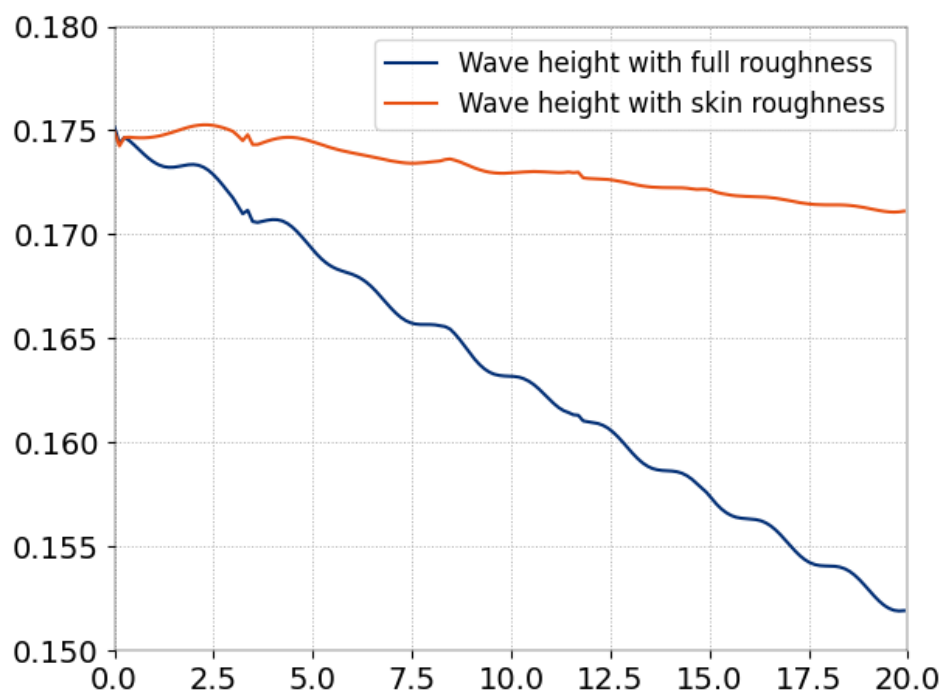


Figure 8.5: Wave height of last calculation on the profile

9. Wave field around a floating body

9.1 Summary

The aim of this test case is to validate the functionality of imposing an incident potential on a boundary. This feature appeared in version 6.2. We compare Artemis with analytical results.

We consider the case of a circular domain with flat bathymetry. At the center of the domain ($x=0$ and $y=0$), a floating body submitted to an incident swell generates a disturbance of the wave field, whose potential Φ_P can be expressed. The center of the simulation is not considered in the simulation. The floating body is taken into account by imposing an incident potential on the inner circle of the fluid domain. This incident potential can be calculated analytically at any distance from the body, providing an analytical reference. The outer circle of the domain is a free output. The results are highly satisfactory.

9.2 Description of the test case

9.2.1 Geometry

The general configuration is described on Figure 9.1 which shows the fluid meshed and its dimension. The bathymetry is flat and the waterdepth is 100m. The inner ray is 50m and the outer ray is 283m No breaking and no friction is taken into account.

The mesh is made with 6912 triangular elements and the nodes are evenly spaced by 5 degrees, with refinement according to the distance to the center.

9.2.2 Boundary conditions

Boundary conditions are given on Figure 9.2

Houle incidente:

- Définie par le potentiel et son gradient :
 - PRBT: Incident potential, real part
 - PIBT: Incident potential, imaginary part
 - DDXPRBT: x-derivative of the incident potential, real part
 - DDYPRBT: y-derivative of the incident potential, real part
 - DDXPIBT: x-derivative of the incident potential, imaginary part
 - DDYPIBT: y-derivative of the incident potential, imaginary part

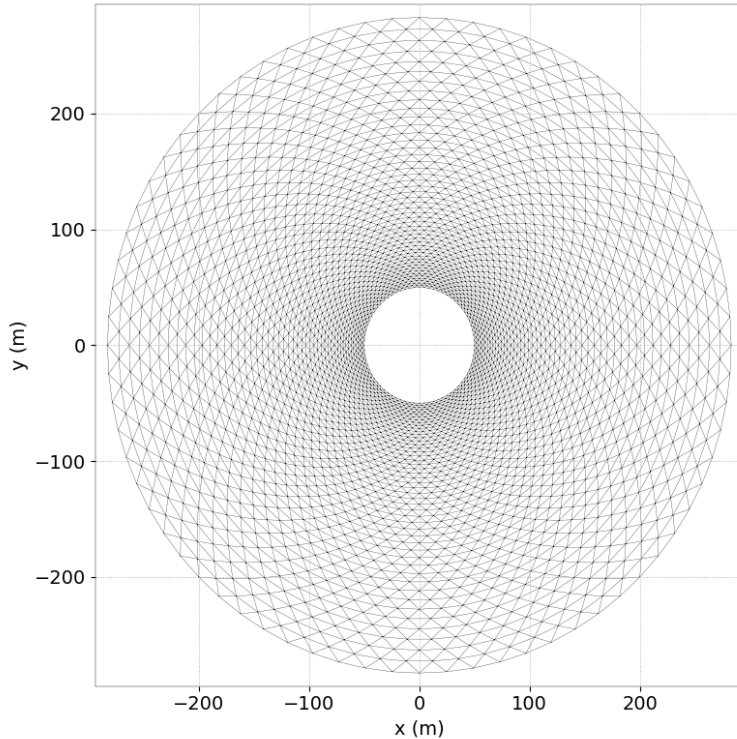


Figure 9.1: Domain of the case

- output direction: 0°
- Incident swell period: 8s

The expression for the incident potential is given by [1]

$$\Phi_{IP} = \sqrt{\frac{k}{2\pi R}} \cdot e^{ikR\frac{\pi}{4}} H(\Theta) \quad (9.1)$$

The z-dependency is given, in accordance with ARTEMIS assumptions, by: $\frac{ch(k(z+d))}{ch(kz)}$
Where

- R is the distance to the centre O (ray in meters).
- Θ is the angle to x-axis.
- k is the wave number.
- d is the water depth

The function $H(\Theta)$ is called Kochin function. In the test case it is written under exponential form:

$$H(\Theta) = Z(\Theta) e^{i\phi(\Theta)}$$

Where Z and Φ are real function read each 5° Gradiants are calculated by finite difference on functions Z and Φ

Free output with an attack angle of 0°

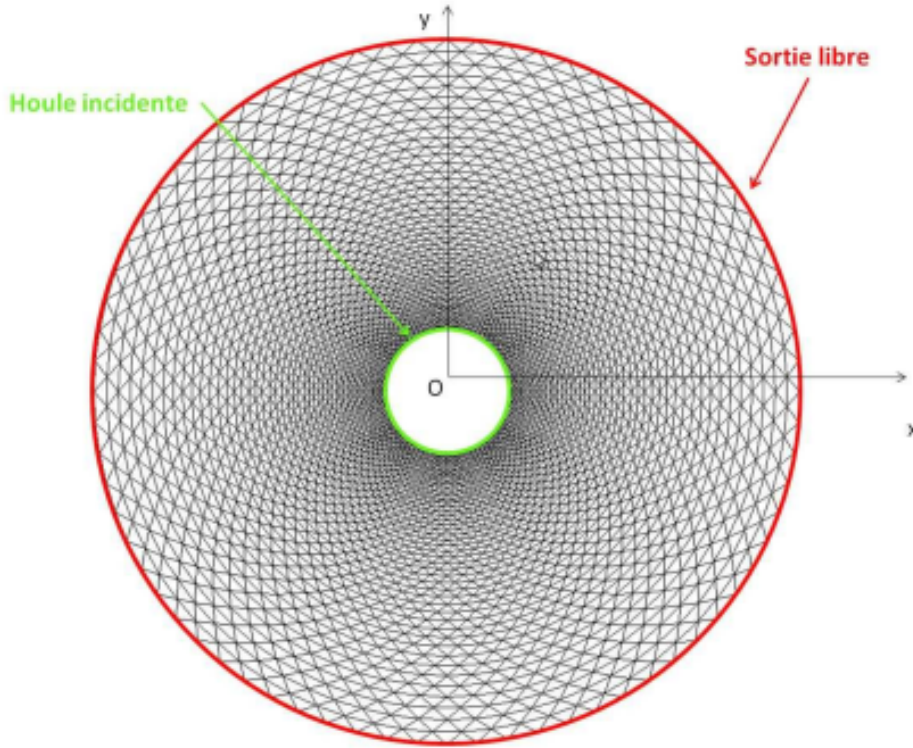


Figure 9.2: Boundary Conditions and orientation

9.3 Reference solution

Φ_P can be calculated at any distance of the centre. This is the reference result. ARTEMIS, for its part, propagates the incident potential entered at $R=50\text{m}$ to the free exit at $R=283\text{m}$. In this area, the result of the Berkhoff equation can be compared with the analytical reference.

9.4 Results

The results obtained with ARTEMIS are shown in Figure 9.3, left-hand column. In the right column, we present the result of the analytical solution. We compare directly The imaginary and real part of the potential from which all other quantities (wave height, free surface, phase ..) depend. The comparison is very satisfactory. An incident potential of any shape is taken into account and its propagation is validated.

9.5 Conclusions

This test case validate that a user can enter an incident swell data other than the "Wave height" and "Propagation direction" data. Any potential can be used.
Radial swell propagation due to the presence of a floating body is also well modelled by ARTEMIS, which is consistent with the analytical solution used for the test case.

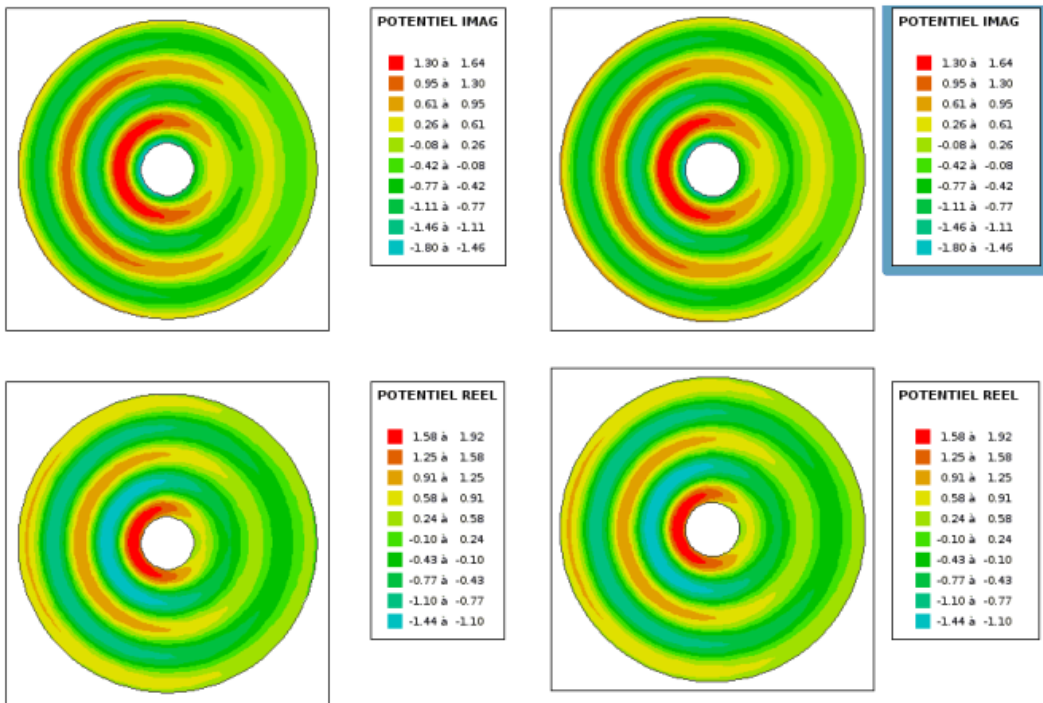


Figure 9.3: Real and imaginary parts of the potential. Comparison between the analytical solution (right) and the ARTEMIS calculation (left) over the entire domain.

10. Schematic port of Delft:port

10.1 Summary

The objective of this test case is to compare Artemis with the results of a physical model of a model of a schematic harbor configuration. The experimentation took place at the Delft Hydraulics Laboratory Hydraulics Laboratory in Delft [1] on a 10m x 8m model. The objective is to validate the port agitation, in particular the taking into account of the reflection on solid boundary.

The results obtained with Artemis are in good agreement with the experimental results.

10.2 Description of the test case

10.2.1 Geometry

The modeled case is included in a rectangle of 10 m by 8 m. The entrance to the harbor is 3 m. The water height is 30 cm and the bathymetry is zero over the whole area.

10.2.2 Mesh

The mesh uses 3265 triangular elements, with a characteristic size of approximately 0.2 m. It is presented in Figure 10.1

10.2.3 Mesh

10.2.4 Boundary conditions

The boundary conditions of the domain are presented in figure 10.2, all are solid wall type except for the harbor entrance, which carries an incident wave condition.

Incidental swell:

- Period = 1.4 s
- Wave height : 0.04 m
- Direction of propagation : 0° .
- Exit direction : 0° .
- Phase (ALFAP) : 0° on the whole boundary

Wall 1:

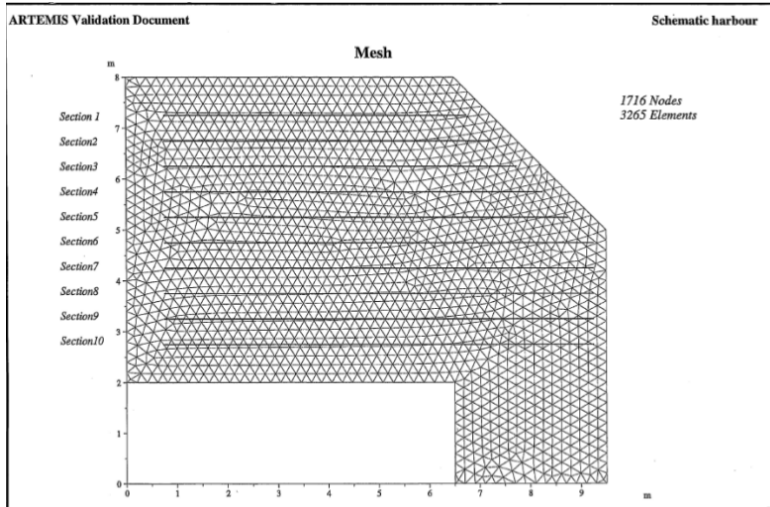


Figure 10.1: Mesh used and measurement planes (sections) for comparisons Experimental/Digital

- Reflection coefficient = 0.23
- Phase shift : 0°
- Angle of attack: 0°

Wall 2:- Reflection coefficient = 1.

- Phase shift : 0°
- Angle of attack: 0° .

Wall 3:

- Reflection coefficient = 1.
- Phase shift : 0°
- Angle of attack : 0° .

Wall 4:

- Reflection coefficient = 0.05
- Phase shift : 0°
- Angle of attack : 45°

Wall 5:

- Reflection coefficient = 0.05
- Phase shift : 0°
- Angle of attack : 0°

Wall 6:

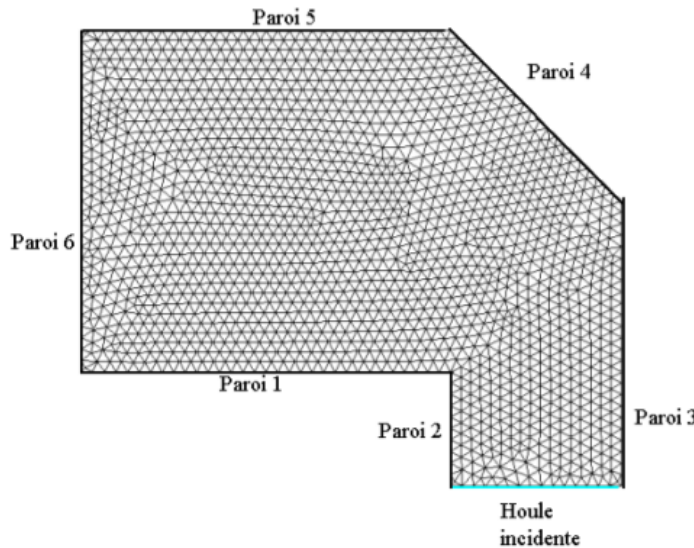


Figure 10.2: Definition of the boundaries

- Reflection coefficient = 0.23
- Phase shift : 0°
- Angle of attack : 0°

We note that a second case has been experimentally realized, with reflection coefficients of 1 on all solid boundaries.

10.3 Reference solution

The results obtained in [12] constitute the reference values, divided into 10 planes. We compare the wave heights obtained numerically and experimentally by presenting the amplification coefficient, defined by :

$$\frac{H(x,y)}{H_{incident}}$$

10.4 Results

The results obtained with Artemis are in good agreement with the experimental results. This shows that the reflection coefficients are well taken into account by Artemis.

10.5 Conclusions

This test case compares Artemis with experimental results on physical model. It allows to validate the modeling of the harbor agitation, and in particular the treatment of reflection coefficients on the solid boundaries in Artemis. The agreement between numerical predictions and the experiment is satisfactory.

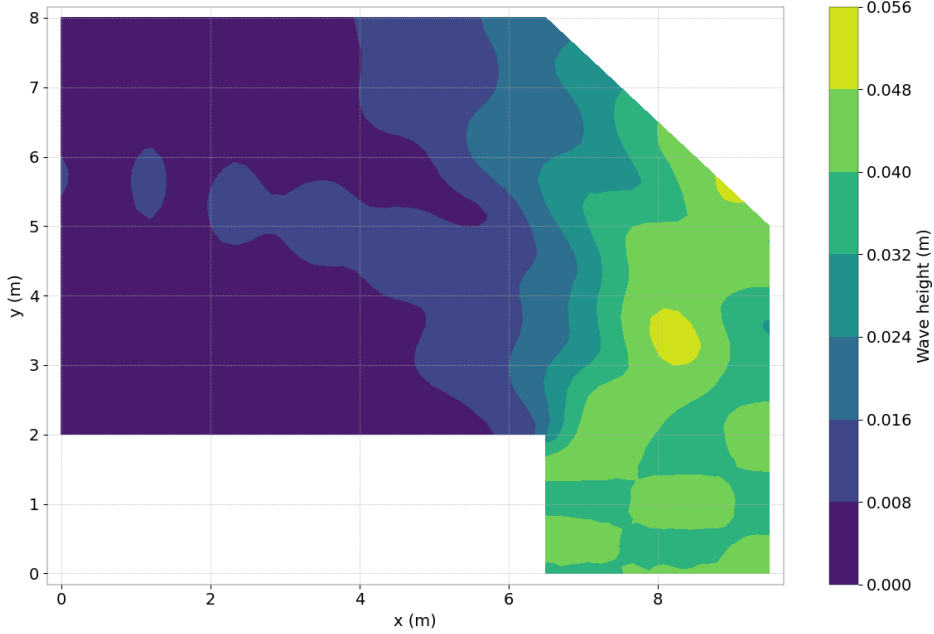


Figure 10.3: Wave height obtained with the last version of ARTEMIS

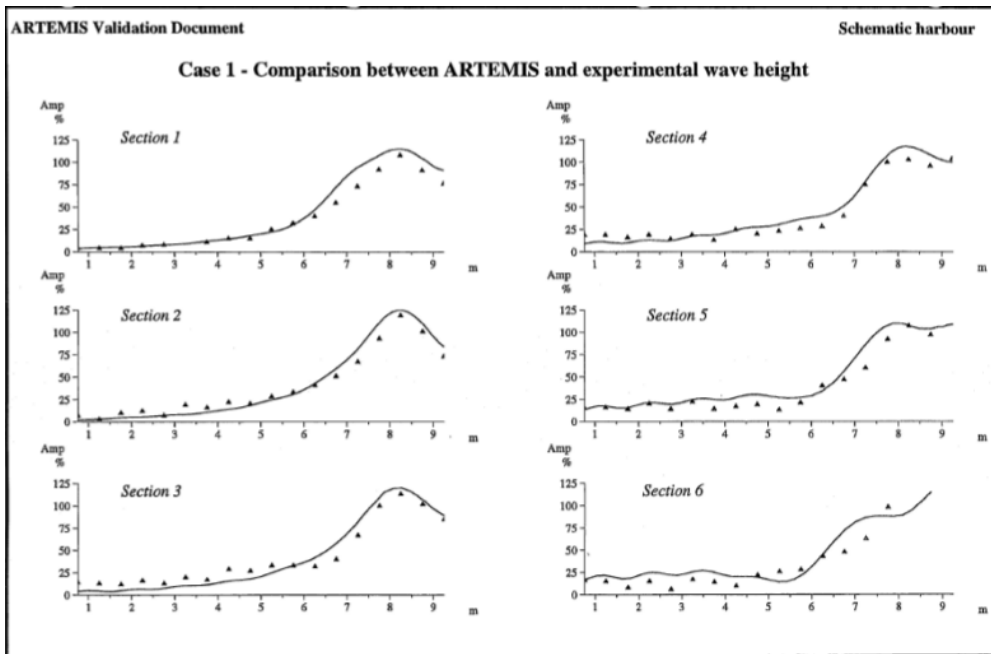


Figure 10.4: dimensionless water heights. Comparison between experimental measurements (triangles) and ARTEMIS (lines)(Rq: results from the validation documents of version 3. update required).

11. Schematic reef: recif

11.1 Summary

The objective of this test case is to validate, on a simple case, the use of the terms of steep slope and curvature terms in the Berkhoff equation (diffraction-refraction equation extended to strong variations of bathymetry, option *RAPIDLY VARYING TOPOGRAPHY* option). Artemis is compared to the results of [15] and REEF2000 [3].

We consider the case of a channel with analytical bathymetry. This case was defined by [15] to represent the configuration of a submerged coral reef, without discontinuity for curvature or slope. It allows to highlight significant deviations between the predictions of the Berkhoff equation alone and the extended Berkhoff equation. We also present the results obtained without the slope and curvature terms in order to validate the treatment of the Berkhoff equation alone.

In both cases, the Artemis results are excellent.

11.2 Description of the test case

The general configuration is described in Figure 11.1, which shows the bathymetry and dimensions of the channel.

Several bathymetries (i.e. "b" values) are tested for validation. They are described in 11.2.1 By default, the test case file sets $b = 2 \text{ m}$. The user is free to modify this value.

The test case is chosen to be as simple as possible, so the calculation does not include either breaking or friction of the bottom.

11.2.1 Geometry

The modeled channel is a 40 m long and 2 m wide rectangle. The bathymetry is set at $z=0$ at the entrance of the channel, then a tangent hyperbolic walk is applied via the following analytical bathymetry.

$$z = \frac{d}{2} \left(1 + \tanh(3\pi(\frac{x-L_1}{b} - 0.5)) \right)$$

The variation of bathymetry is thus mainly on the domain "b", outside it is negligible.

We vary b from 20 cm to 20 m to appreciate the impact of the slope and curvature terms. The coast of the free surface is 6m.

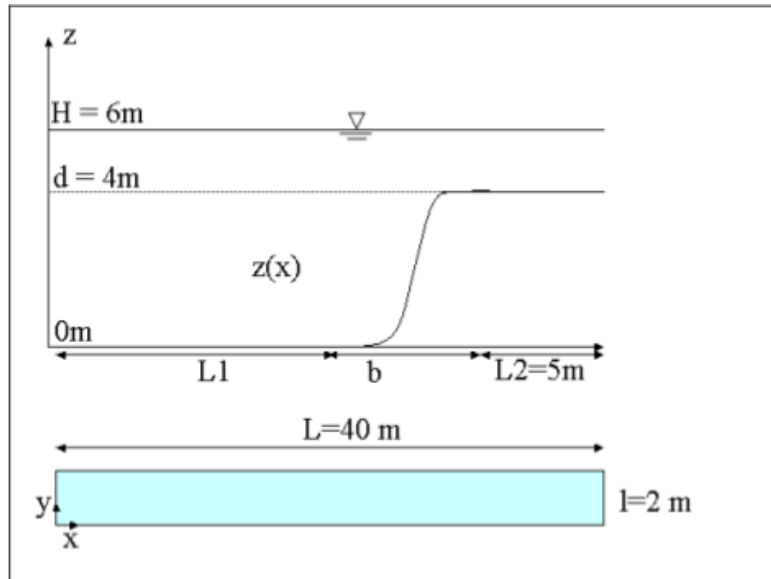


Figure 11.1: Configuration of the problem

11.2.2 Mesh size

The mesh used is an adjusted mesh generated by Janet. It consists of 400 000 triangular elements. The nodes are regularly spaced by 2 cm on the x-axis and y-axis.

11.2.3 Boundary conditions

The boundary conditions of the domain are presented in Figure 11.2.



Figure 11.2: Boudary conditions

Incident swell:

- Period = 6.34 s
- Wave height : 0.05 m
- Propagation direction: 0° .
- Exit direction: 0° .
- Phase (ALPHAP): 0° on the whole liquid boundary

Wall:

- Reflection coefficient = 1.
- Phase shift: 0°
- Angle of attack: 0°

Free exit:

- Angle of attack of the outgoing waves: 0° .

11.3 Reference solution

The results obtained by [15] constitute the reference points for the following values of b values: 0.4m, 0.5m, 1m, 2m, 4m, 8m.

In [3], we find curves describing all values of b in the interval [0.2m ;20m].

In these two references, the results obtained with the simple Berkhoff equation and with the extended Berkhoff equation are presented. The comparison criterion used is the reflection coefficient, which we define as follows:

$$C_{Reflexion} = \frac{H_{max} - H_{incident}}{H_{incident}}$$

with $H_{incident}$ the incident wave height and H_{max} the maximum wave height observed in the resulting wave field (incident +reflected)

11.4 Results

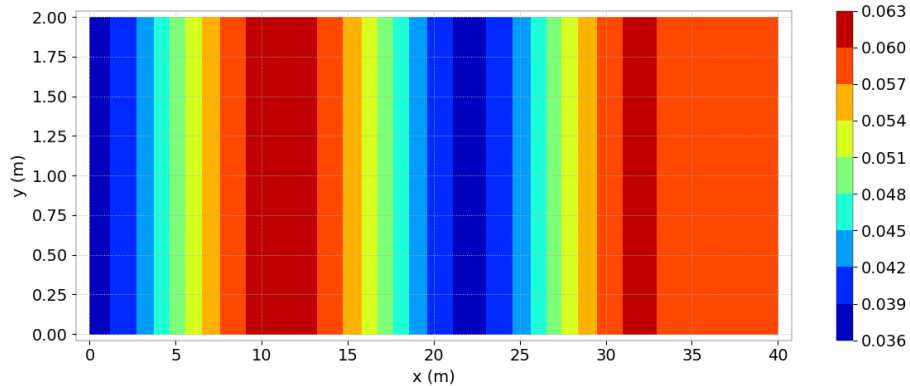


Figure 11.3: wave height for $b=4m$

The results obtained with Artemis are in very good agreement with the two references bibliographic references (numerical). This is true for the Berkhoff equation alone or the extended equation taking into account the effects of slope and curvature.

11.5 Conclusions

This test case allowed us to compare Artemis to other codes solving the Berkhoff equation equation with or without taking into account slope and curvature effects. The results are excellent: Artemis gives results very close to the two other codes on the whole range of cases studied.

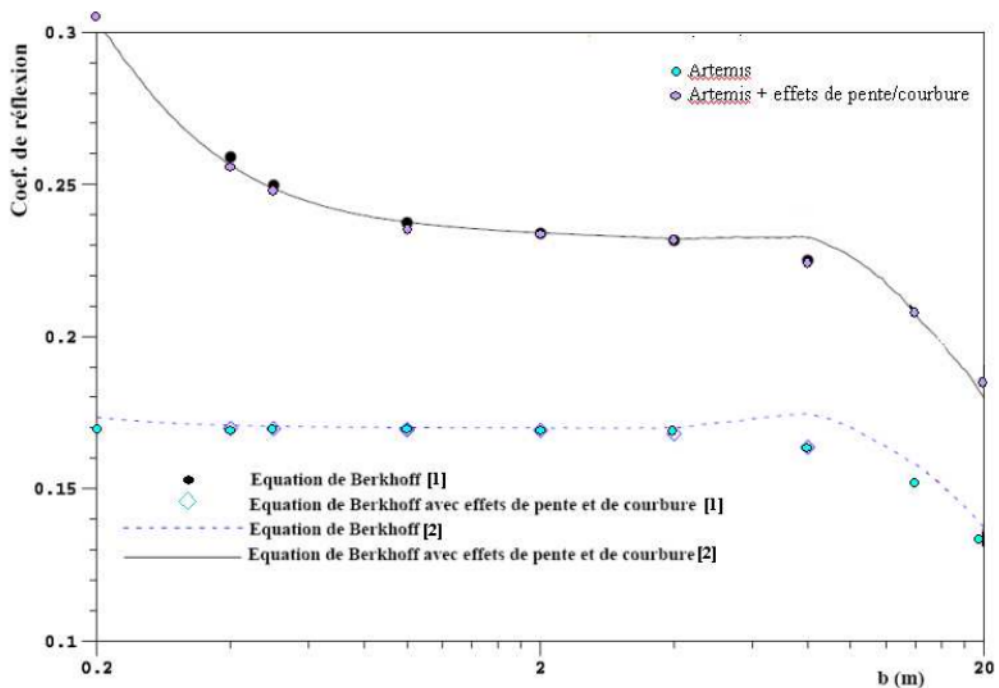


Figure 11.4: Reflection coefficients as a function of bathymetry (length b of the reef). Comparison between ARTEMIS (blue and grey points) with references [3] (black points, blue diamonds) and [15] (blue and black lines)

12. Reflection on rippled bottom: rides

12.1 Summary

The objective of this test case is to analyze the wave behavior related to a rippled bathymetry. We take the opportunity to underline the interest of taking into account the terms of slope and curvature in the Berkhoff equation (extended diffraction-refraction equation, option *RAPIDLY VARYING TOPOGRAPHY*). Artemis is compared to experimental results [8] and numerical results [3].

We consider the case of a channel with analytical bathymetry. This case was defined by [8] to study the phenomenon of reflection for a swell propagating on a rippled bottom. The rippled bottom takes the form of 10 periods of a sine function. The interest of this case, besides proposing an experimental reference, is to be a discriminating case between predictions of the Berkhoff equation alone and predictions of the extended equation.

Results without the slope and curvature terms are also presented. This allows us to compare our values with the numerical results of [3], and to show the interest of taking into account the slope and curvature terms.

The results are satisfactory and show the good agreement between the numerical prediction and the experimental results.

12.2 Description of the test case

The general configuration is described in Figure 12.1, which presents the bathymetry and dimensions of the channel. The detailed bathymetry can be found in 12.2.1.

Several wave frequencies are tested for validation. They are described in 12.2.3. By default, the test case file sets the wave period to $T = 1.3$ s. The user is free to modify this value. The test case is chosen as simple as possible, so the calculation does not include neither breaking nor bottom friction.

12.2.1 Geometry

The modeled channel is a 40 m long and 2 m wide rectangle.

The bathymetry is fixed at $z=0$ from the channel entrance to $x=L_1=25$ m. Then it takes the form of a sine function:

$$\text{For } L_1 < x < L_1 + b \quad z = A \sin\left(\frac{2\pi}{\lambda_b}(x - L_1)\right)$$

with

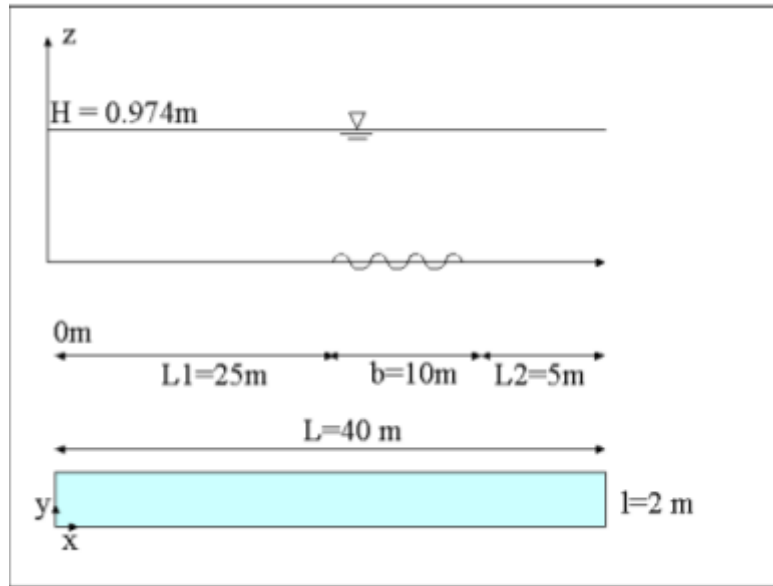


Figure 12.1: Configuration of the problem

- $A = 0.05\text{m}$
- $\lambda_b = 1\text{m}$
- $L_1 = 25\text{m}$

The coast of the free surface is 0.313m.

12.2.2 Mesh

The mesh used is an adjusted mesh generated by Janet. It consists of 400 000 triangular elements. The nodes are regularly spaced by 2 cm on the x-axis and y-axis.

12.2.3 Boundary conditions

The boundary conditions of the domain are presented in Figure 12.2.

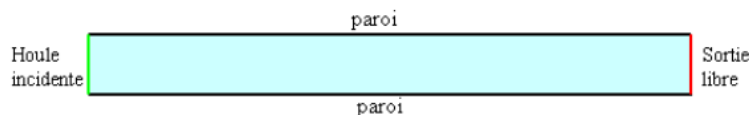


Figure 12.2: Boundary conditions

Incidental swell:

- Period = variable [0.974 s; 2.37 s]
- Wave height : 0.01 m
- Propagation direction: 0°
- Exit direction: 0° .

- Phase (ALFAP): 0° on the whole liquid boundary

Wall:

- Reflection coefficient = 1.
- Phase shift: 0°
- Angle of attack: 0°

Free exit:

- Angle of attack of the outgoing waves: 0° .

12.3 Reference solution

The experimental results proposed in [8] constitute data over a wide range of frequency range. They are presented as reflection coefficients as a function of:

$$\frac{2\lambda_b}{\lambda_{swell}}$$

where λ_{swell} is the wavelength of the swell function of the chosen period. In [3] we find curves related to this configuration. The results are presented with a Berkhoff approach alone and also taking into account the effects of slope and curvature effects.

Artemis is compared with these two references. The comparison criterion is the reflection coefficient, which we define as follows:

$$C_{Reflexion} = \frac{H_{max} - H_{incident}}{H_{incident}}$$

with $H_{incident}$ the incident wave height and H_{max} the maximum wave height observed in the resulting wave field (incident +reflected)

12.4 Results

The results obtained with Artemis are in good agreement with the experimental reference. In particular we can see that the peak of the reflection coefficient for $2\lambda_b/\lambda_{swell} = 1$ is much better predicted by the extended Berkhoff equation than by the Berkhoff equation alone.

Code-to-code comparison with REEF2000 gives an excellent agreement.

12.5 Conclusions

The experimental results are well reproduced in a qualitative way, and are satisfactory quantitatively. The comparison with the REEF2000 code shows an excellent correlation. This allows in particular to validate the option *RAPIDLY VARYING TOPOGRAPHY* option of the code.

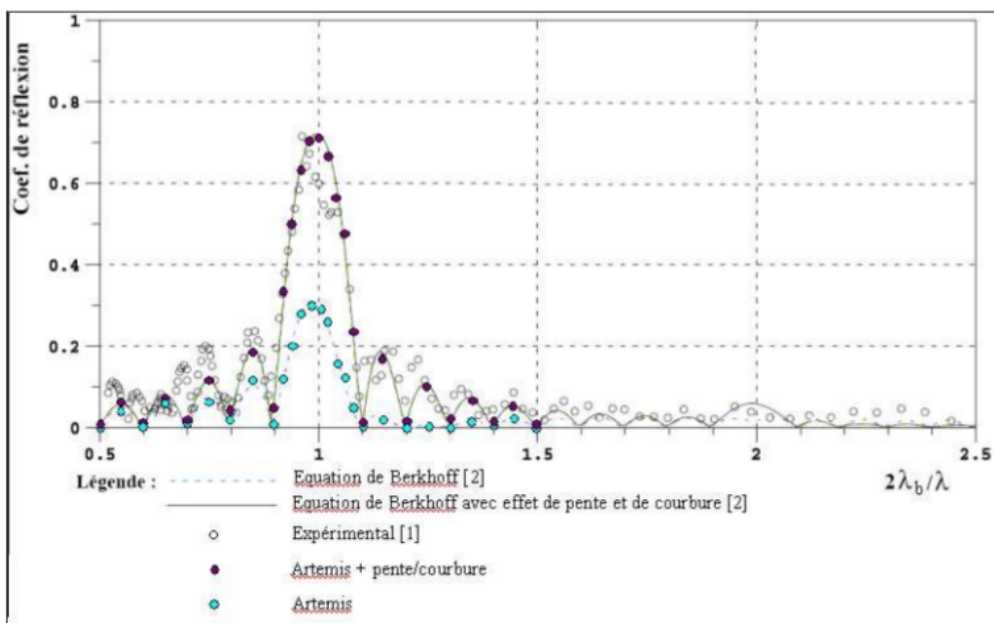


Figure 12.3: Reflection coefficients as a function of bathymetry (ripple wavelength). Comparison between ARTEMIS (blue and violet dots) with the experiment (white point) [3] (black line)

[9]

- [1] Aurelien Babarit. Wave field around a floating body using far field approximation. Technical report, 2011.
- [2] J.A. BATTJES and J.P.F.M. JANSSEN. Energy loss and set-up due to breaking of random waves. In *Proc. 16th Int. Conf. Coastal Eng.*, pages 569–587., 1978.
- [3] Michel Benoit. Extension de l'équation de réfraction-diffraction de berkhoff pour traiter des bathymétries rapidement variables. développement et validation d'un algorithme applicableaux cas monodimensionnels pour une houle linéaire. Technical Report HE-42/99/049/A., EDF, 1999.
- [4] C.E.R.C. Shore protection manual. volumes i and ii, 4th ed. s.l. : US Army Corps of Engineers, 1984.
- [5] CERC. *Shore Protection Manual Volume 1*. USACE, Vicksburg, MS, 1984.
- [6] C.N. Chandrasekera and K.F. Cheung. Extended linear refraction-diffraction model. *Journal of Waterway, Port, Coastal and ocean engineering*, 123:280–286, 1997.
- [7] Dean R.G. Dally, W.R. and R.A. Dalrymple. A model for breaker decay on beaches. s.l. : Engineering, 19th International Conference on Coastal, 1984.
- [8] Heathershaw A.D. Davies A.G. Surface wave propagation over sinusoidally varying topography. *J. Fluid Mech.*, 1984.
- [9] J-M. HERVOUET. *Hydrodynamics of free surface flows. Modelling with the finite element method*. John Wiley & Sons, Ltd, Paris, 2007.
- [10] Bowen A.J. Inman D.L. Flume experiments on sand transport by waves and currents. *I.C.C.E.*, 11:137–150, 1962.
- [11] Berkhoff J.C.W. Wave deformation by a shoal. comparison between computations and mesurements. report on a mathematical investigation w154 part viii. Technical report, Delft Hydraulics Laboratory, march 1982.
- [12] Delft Hydraulics Laboratory. Wave penetration into harbours.comparison of computation and model measurement. *Delft Hydraulics Laboratory*, 154, 1981.
- [13] Van Rijn L.C. Principles of sediment transport in rivers, estuaries and coastal seas. *Aqua Publications*,, 1993.
- [14] Yoon SB Lee C. Effect of higher-order bottom variation terms on he refraction of water waves in the extended mild-slope equations. *Ocean engineering*, 2004.

- [15] Massel. Extended refraction-diffraction equation for surface waves. *Coastal Eng.*, 19: 97–126, 1993.
- [16] Stive M.J.F. Energy dissipation in waves breaking on gentle slopes. *Coastal Engineering*, (8):99–127, 1984.
- [17] J.A. Putnam and J.W. Johnson. The dissipation of wave energy by bottom friction. *1949. pp. 67-74.*
- [18] Johnson J.W. Putnam J.A. The dissipation of wave energy by bottom friction. *Transactions, American Geophysical Union*, 30:67–74, 1949.
- [19] Holmes P. Williams RG, Darbyshire J. Wave refraction and diffraction in a caustic region : a numerical solution and experimental validation. *Proc. Inst. Civil Engrs.*, 1980.